The Cryosphere Discuss., 5, 3541–3594, 2011
www.the-cryosphere-discuss.net/5/3541/2011/
doi:10.5194/tcd-5-3541-2011

The Cryosphere Discussions

A new glacier inventory for 2009 reveals spatial and temporal variability in glacier response to atmospheric warming in the Northern Antarctic Peninsula, 1988–2009

B. J. Davies[1], J. L. Carrivick[2], N. F. Glasser[1], M. J. Hambrey[1], and J. L. Smellie[3]

[1]Centre for Glaciology, Institute for Geography and Earth Sciences, Aberystwyth University, Llandinam Building, Penglais Campus, Aberystwyth SY23 3DB, UK
[2]Department of Geography, University of Leeds, Leeds LS2 9JT, UK
[3]Department of Geology, University of Leicester, Leicester LE1 7RH, UK

Received: 2 December 2011 – Accepted: 8 December 2011 – Published: 21 December 2011

Correspondence to: B. J. Davies (bdd@aber.ac.uk)

Published by Copernicus Publications on behalf of the European Geosciences Union.

Abstract

The Northern Antarctic Peninsula has recently exhibited ice-shelf disintegration, glacier recession and acceleration. However, the dynamic response of land-terminating, ice-shelf tributary and tidewater glaciers has not yet been quantified or assessed for variability, and there are sparse published data for glacier classification, morphology, area, length or altitude. This paper firstly uses ASTER images from 2009 and a SPIRIT DEM from 2006 to classify the area, length, altitude, slope, aspect, geomorphology, type and hypsometry of 194 glaciers on Trinity Peninsula, Vega Island and James Ross Island. Secondly, this paper uses LANDSAT-4 and ASTER images from 1988 and 2001 and data from the Antarctic Digital Database (ADD) from 1997 to document glacier change 1988–2009. From 1988–2001, 90 % of glaciers receded, and from 2001–2009, 79 % receded. Glaciers on the western side of Trinity Peninsula retreated relatively little. On the eastern side of Trinity Peninsula, the rate of recession of ice-shelf tributary glaciers has slowed from 12.9 $km^2 a^{-1}$ (1988–2001) to 2.4 $km^2 a^{-1}$ (2001–2009). Tidewater glaciers on the drier, cooler Eastern Trinity Peninsula experienced fastest recession from 1988–2001, with limited frontal retreat after 2001. Land-terminating glaciers on James Ross Island also retreated fastest in the period 1988–2001. Large tidewater glaciers on James Ross Island are now declining in areal extent at rates of up to 0.04 $km^2 a^{-1}$. This east-west difference is largely a result of orographic temperature and precipitation gradients across the Antarctic Peninsula. Strong variability in tidewater glacier recession rates may result from the influence of glacier length, altitude, slope and hypsometry on glacier mass balance. High snowfall means that the glaciers on the Western Peninsula are not currently rapidly receding. Recession rates on the eastern side of Trinity Peninsula are slowing as the floating ice tongues retreat into the fjords and the glaciers reach a new dynamic equilibrium. The rapid glacier recession of tidewater glaciers on James Ross Island is likely to continue because of their low elevations and flat profiles. In contrast, the higher and steeper tidewater glaciers on the Eastern Antarctic Peninsula will attain more stable frontal positions after low-lying ablation areas are removed.

1 Introduction

The Northern Antarctic Peninsula Ice Sheet is particularly dynamic and sensitive to climate change because of its relatively small size and northern location (Vaughan et al., 2003; Smith and Anderson, 2010). The Antarctic Peninsula region is also one of the most rapidly warming places on Earth, with mean air temperature increasing by 2.5 °C over the last 50 yr (King, 1994; Turner et al., 2005). With continued atmospheric warming predicted for the Antarctic Peninsula region over the next century (Vaughan et al., 2003), the viability of glaciers in this region is questionable. With this warming trend, the −9 °C annual isotherm (the thermal limit of ice shelves (Morris and Vaughan, 2003)) has moved southwards, resulting in 28 000 km^2 being lost from Antarctic Peninsula ice shelves since 1960 (Vaughan and Doake, 1996; Cook et al., 2005; Cook and Vaughan, 2010). Ice-shelf tributary glaciers accelerated and thinned following the disintegration of Larsen Ice Shelf (De Angelis and Skvarca, 2003), with up to a six-fold increase in centre-line speeds (Scambos et al., 2004). Other tidewater glaciers on the Antarctic Peninsula are accelerating, thinning and retreating in response to increased atmospheric and sea surface temperatures (Pritchard and Vaughan, 2007). Antarctic Peninsula glaciers currently contribute 0.22 ± 0.16 mm a^{-1} to sea level rise (Hock et al., 2009), and have a total eustatic sea-level equivalent of 0.24 m (Pritchard and Vaughan, 2007). It is clearly important to establish how the on-going mass balance changes and associated thinning, drawdown and ice front retreat will progress, and how these changes will impact future on sea level.

Glacier inventory mapping is an essential prerequisite for regional mass balance studies and for modelling future glacier extents (Abermann et al., 2009). It is therefore surprising, given the glaciological responses to climate change outlined above, that a detailed and up-to-date glacier inventory does not exist for the Northern Antarctic Peninsula (Racoviteanu et al., 2009; Leclercq et al., 2011). Previous inventories have focussed on changes up to 2001, and contain few quantitative data suitable for inventory and numerical modelling purposes (Rabassa et al., 1982; Skvarca et al., 1995; Rau

et al., 2004). What is particularly lacking is data on how glaciers have responded to climate change across the Northern Peninsula on a local scale; i.e. with respect to the varied geological, climatic and glaciological settings. For example, there are outstanding questions regarding how the tributary glaciers on James Ross Island and Northeast Antarctic Peninsula have changed since the 1995 disintegration of Prince Gustav Ice Shelf (PGIS) (cf., Rott et al., 1996; Glasser et al., 2011), and the likely future behaviour of these glaciers. Since PGIS was the first regional ice shelf to disintegrate on the Eastern Antarctic Peninsula, the comparatively long time elapsed since that event offers an unusual opportunity to analyse the consequential response of tidewater and ice-shelf tributary glaciers to ice shelf removal.

This paper aims to create an inventory of the glaciers of Trinity Peninsula, James Ross Island and Vega Island (Fig. 1). Our comprehensive survey includes not only glacier length and area, as in previous inventories of James Ross Island (cf., Rabassa et al., 1982; Skvarca et al., 1995; Rau et al., 2004), but also coordinates, glacier geometry, geomorphology, elevation, aspect, slope, hypsometry, equilibrium line altitude (ELA), width of calving front, terminal environment, snow coverage and topographic context. Secondly, we use this new dataset to analyse change in glacier extent between 1988, 1997, 2001 and 2009. These parameters provide the basis for the first comprehensive and holistic understanding of changes in Antarctic Peninsula ice shelves, tributary glaciers, tidewater glaciers and land-terminating glaciers over the past two decades. This paper therefore has five specific objectives: (i) to map the length and extent of each individual glacier in 1988, 1997, 2001 and 2009; (ii) to identify parameters for each glacier in line with the GLIMS (Global Land Ice Measurements from Space; www.glims.org) programme (cf., Racoviteanu et al., 2009); (iii) to establish rates of recession for these glaciers from 1988 to 2009; (iv) to analyse spatial and temporal variability in recession rates, and (v) to determine controls upon recession rates.

2 Regional setting

2.1 Location and climate

Trinity Peninsula is the northernmost part of Graham Land, Northern Antarctic Peninsula (Fig. 1). The region of interest for this paper extends from Cape Dubouzet (63° S, 57° W) to Larsen Inlet (64° S, 59° W). James Ross Island is separated from the Antarctic Peninsula by Prince Gustav Channel, which is 8 to 24 km wide (Fig. 1). Water depths reach 1200 m and shallow southwards to less than 450 m (Evans et al., 2005). The north-south orientated Antarctic Peninsula mountains are an orographic barrier to persistent Southern Ocean westerlies. Cold continental air in the Weddell Sea also flows northwards, barring the warmer maritime air masses of the Bellingshausen Sea (King et al., 2003). The Western Antarctic Peninsula therefore has a polar maritime climate, dominated by the warm Bellingshausen Sea, whilst the Eastern Antarctic Peninsula and James Ross Island have a polar continental climate, dominated by the Weddell Sea (Martin and Peel, 1978; Vaughan et al., 2003). The western coast of the Antarctic Peninsula is therefore typically 7 °C warmer than the eastern coast. These differences are further exacerbated by the different sea-ice regimes in the Bellingshausen and Weddell seas, with the Weddell Sea being sea-ice bound for much of the year (King et al., 2003).

Climate records from the South Orkney Islands suggest that regional warming probably began in the 1930s (Vaughan et al., 2003). The greatest warming rates are in the east (at Marambio and Esperanza stations; cf. Fig. 1), and the smallest on the northwest coast. The most pronounced warming is in the winter months, and is related to changes in atmospheric circulation, sea ice extent and ocean processes (Stastna, 2010). The Antarctic Oscillation represents the periodic strengthening and weakening of the belt of tropospheric westerlies that surround Antarctica (van den Broeke and van Lipzig, 2004). A strengthening of this circumpolar vortex results in an asymmetric surface pattern change, with pressure falling over Marie Byrd Land. This pressure pattern causes northerly flow anomalies, which in turn produce cooling over East Antarctica

and warming over the Antarctic Peninsula. Decreased sea ice in the Bellingshausen Sea enhances warming over the Western Peninsula and the Weddell Sea. This is associated with decreases in precipitation over the South-Western Peninsula (van den Broeke and van Lipzig, 2004), but the Western Peninsula in general has the greatest precipitation rates in Antarctica, typically 3–4 times that of any other part of the continent (van Lipzig et al., 2004). Since the 1950s, the Antarctic Circumpolar Current has warmed by 0.2 °C, with the warming greatest near the surface (Gille, 2008), and waters to the west of the Antarctic Peninsula have warmed very rapidly (Turner et al., 2005; Mayewski et al., 2009).

2.2 Contemporary glaciology

The Antarctic Peninsula Ice Sheet is typically 500 m thick over Trinity Peninsula, and its central plateau glaciers attain altitudes of over 1600 m a.s.l. along its central spine (Fig. 1). Trinity Peninsula outlet glaciers flow predominantly east and west, perpendicular to the Peninsula spine (Heroy and Anderson, 2005). On the eastern flank many outlet glaciers terminate in floating or partly floating tongues. The North-Western Trinity Peninsula coastline mainly comprises grounded ice cliffs with the floating ice margins of a few small ice shelves and numerous small glaciers (Ferrigno et al., 2006).

Currently, 80 % of James Ross Island is ice-covered (Rabassa et al., 1982), with the remainder comprising rock or Quaternary sediments with perennial permafrost (Fukuda et al., 1992). The island is bounded to the Southwest, South and East by high cliffs and valley glaciers, and the ice cap drains over the cliffs into outlet glaciers, principally via avalanches and ice falls (Skvarca et al., 1995). The bedrock structure of resistant volcanic rocks overlying soft Cretaceous sediments (Smellie et al., 2008; Hambrey et al., 2008) fosters the development of elongate, over-deepened cirques, with steep or near vertical back walls up to 800 m high. Vega Island is dominated by two plateau ice caps that feed numerous small tidewater glaciers. The ice-free area (approximately 34 %) is dominated by permafrost processes. Snow Hill Island, Corry Island and Eagle Island (Fig. 1) are dominated by large marine-terminating glaciers.

Snow Hill Island has extensive floating margins.

Retreating tidewater termini have been mapped for the entire Trinity Peninsula, with outlet glaciers on James Ross Island showing large reductions in area since the 1940s (Ferrigno et al., 2006). PGIS was connected to Larsen Ice Shelf until 1957/58 (Cook and Vaughan, 2010). The northernmost ice shelf on the Eastern Antarctic Peninsula, it was the first to show signs of retreat (Ferrigno et al., 2006), and rapidly disintegrated in 1995 (Skvarca et al., 1995; Cooper, 1997), followed by the thinning, acceleration and rapid recession of the former ice shelf feeding glaciers (Rau et al., 2004; Glasser et al., 2011). During the later twentieth century, most glaciers on James Ross Island and North-Eastern Antarctic Peninsula experienced rapid recession and calving, with the strongest evidence of recession in the northernmost parts. This is generally attributed to prevailing climatic warming (Vaughan et al., 2003; Rau et al., 2004). An average retreat rate of the James Ross Island glaciers of 1.8 $km^2 a^{-1}$ from 1975–1988 (Skvarca et al., 1995) doubled after the disintegration of PGIS, to 3.8 $km^2 a^{-1}$ between 1988 and 2001 (Rau et al., 2004). Although Skvarca et al. (1995) noticed no dramatic change for small land-based glaciers from 1977 to 1988, retreat was observed from 1988 to 2001 (Skvarca et al., 1995; Skvarca and De Angelis, 2003).

3 Data sources and methods

3.1 2009 glacier inventory

3.1.1 Data sources

This inventory is a snapshot of the glaciers on Trinity Peninsula, James Ross Island, Snow Hill Island and Vega Island in 2009. This data has been made available for download from the GLIMS geodatabase. Our methods conform to those set out by the GLIMS programme (Racoviteanu et al., 2009), and are given in full in the Supplement. Mapping was conducted in ArcGIS 9.3 from interpretation of 2009

ASTER images (Table 1 and Supplement). The geographical area mapped was limited by the availability of satellite imagery). The Antarctic Digital Database (ADD, http://www.add.scar.org:8080/add/) Coastal Change dataset (from Cook et al., 2005) was used to provide additional data where the ice margin was difficult to map (e.g., because of high cloud cover). Topographic elevation data and contours were derived from the 2006 SPIRIT Digital Elevation Model (DEM) (Table 1). Ground-control points were not necessary since accurate geolocation of the SPOT-5 images is possible. Each pixel in a SPOT-5 image can be located on the ground to ±25 m at the 66 % confidence interval, although errors may be larger in areas of flat glacier ice (Reinartz et al., 2006; Berthier et al., 2007; Korona et al., 2009). Glacier names and numbers were taken from previous glacier inventories and published maps (Rabassa et al., 1982; British Antarctic Survey, 1995, 2010; Czech Geological Survey, 2009).

3.1.2 Error estimation

Sources of uncertainty and mitigation strategies are summarised in Table 2. The largest errors in glacier drainage basin delineation are derived from interpreter error of ice-divide identification and mapping. DEM quality in areas of flat white ice also limits the accuracy of ice divide mapping. ASTER Level 1B images are pre-processed but were co-registered to the SPOT-5 images to reduce errors. Calculation of area is limited by the pixel resolution of the dataset (i.e. ±15 m for ASTER images). Mapping was estimated to be accurate to within 3 pixels (i.e. 45 m). A buffer of 22.5 m width was therefore placed either side of each glacier polygon, providing a minimum and maximum estimate of size and a total error margin equivalent to 3 pixels. There may also be an error in ASTER co-registration (Granshaw and Fountain, 2006); but this is assumed to be within the mapping limits.

3.1.3 Drainage basin delineation

Automated methods for large-scale inventories can be used to map large regions quickly (e.g., Svoboda and Paul, 2009; Bolch et al., 2010), but they do not allow such high detail in digitisation. For this reason, we used manual digitisation to establish glacier polygons in our high-resolution study of a small region, following guidelines set out by the GLIMS programme (refer to Supplement). A glacier polygon is a coherent body of ice that includes all tributaries and connected feeders, and excludes exposed ground and nunataks (Racoviteanu et al., 2009; Raup and Khalsa, 2010). On James Ross Island many glaciers have well defined cirques, but the plateau above them was included in their polygons (Fig. 1); this is because ice situated above the cliff-backed bergschrund contributes snow and ice through frequent avalanches and creep flow to the glacier.

3.1.4 Attribute data for glacier drainage basins

Attribute information determined for each glacier polygon comprises *Area, Length, Coordinates, Name* (if published), *Glacier ID* (e.g., GAP17 or GIJR65, standing for Glacier Antarctic Peninsula and Glacier James Ross Island, respectively; these conform where appropriate to previous inventories), *GLIMS ID, Elevation, Width of calving front, Date of scene acquisition, Satellite, Tongue* (grounded, floating, land-terminating), *Primary classification, Form, Frontal characteristics, Moraines, Debris on tongue, Remarks, Slope, Aspect, ELA* and *Hypsometry*, in addition to notes on geomorphology and glaciology (cf., Rau et al., 2005; Raup et al., 2007a,b; Racoviteanu et al., 2009; Paul et al., 2010; Raup and Khalsa, 2010). *Form, Primary Classification, Frontal Characteristics* and *Remarks* are geomorphological descriptors that provide detailed information on the glaciers shape, terminus and classification (e.g., cirque, niche, outlet, valley glaciers) that correspond to GLIMS guidelines (Rau et al., 2005; Paul et al., 2010).

In the *Tongue* parameter, glaciers were categorised as floating, partially floating, grounded or land-terminating. Land-terminating glaciers are relatively few in Antarctica,

but as their recession is controlled more directly by changes in atmospheric temperature and precipitation than marine-terminating glaciers, they can be a sensitive indicator of climate change (Oerlemans, 2005; Carrivick et al., 2011). The nature of the marine-terminating glacier tongue has important implications for oceanographic and glaciological applications, but the grounding zone can only be accurately located with detailed geophysical surveys (Brunt et al., 2010), which are impractical for glacial inventories. However, the floating tongues of marine-terminating glaciers typically have several visual characteristics in common: a pronounced break in slope at the grounding-line, an irregular, heavily crevassed and convex calving front, a flat long profile, an irregular margin, and occasional large rifts. Alternatively, grounded tidewater glaciers are typically characterised by a concave calving front, a steadily dipping long profile, and have no clear break in slope (Dahl and Nesje, 1992; Scambos et al., 2004; Reinartz et al., 2006; Lambrecht et al., 2007; Fricker et al., 2009). Marine-terminating glaciers that exhibit a combination of these characteristics are defined as partially floating, where either it is difficult to determine whether a glacier is floating or not, or where the glacier may be grounded at the lateral margins but floating in the centre of the calving margin.

Data were automatically derived in the GIS for minimum (H_{MIN}), maximum (H_{MAX}), mean (H_{MEAN}) and median (H_{MEDIAN}) elevation using the 2006 SPIRIT DEM. Elevation data are unavailable for GAP40, GAP43 and glaciers north of GAP34 because of the geographical limits of the SPIRIT DEM. Values for mean slope and aspect were also calculated for each glacier polygon using the 2006 SPIRIT DEM (refer to Supplement). Aspect and slope are useful data for modelling purposes (Paul et al., 2010), and mean slope can be used as a proxy for ice thickness.

3.1.5 Glacier hypsometry

Glacier hypsometry is the distribution of glacier surface area with altitude, and is a major control on mass balance, as it strongly determines the accumulation area ratio (AAR) of a glacier. It is dependent on valley shape, topographic relief and glacier

depth. When the ELA of a glacier changes, for example due to climate change, the extent of the impact on the glacier relies on the glacier hypsometry (Furbish and Andrews, 1984). Faster rates of accumulation area loss during climatically-driven ELA rise will result in increased glacier recession. Glacier hypsometric curves were calculated by masking 54 glacier polygons (i.e. those over 40 km^2; all tidewater outlet glaciers) with the SPIRIT DEM, and the area in each 100 m elevation bin was calculated. Hypsometric curves of cumulative area (km^2) could then be plotted for the largest glaciers. A single Hypsometric Index (HI) (equivalent to "altitude skew") was calculated for each glacier polygon using the equation below, originally presented by Jiskoot et al. (2009), where

$$\mathrm{HI} = \frac{H_{median} - H_{max}}{H_{median} - H_{min}}, \quad \text{and if} \quad 0 < \mathrm{HI} < 1, \quad \text{then} \quad \mathrm{HI} = \frac{-1}{\mathrm{HI}}$$

3.1.6 Equilibrium line altitude derivation

In a glacier inventory, an estimation of the mean long-term ELA is considered to be vital, because it divides a glacier into ablation and accumulation areas. If air temperature rises and/or if there is declining effective accumulation, mass balance will decline and the ELA will rise. ELAs have considerable inter-annual variability, with positive and negative mass balances from one year to the next (e.g., Carrivick and Chase, 2011). The long-term ELA is best determined by a programme of mass-balance measurements over several years (Braithwaite and Raper, 2009). However, field programmes are time consuming and expensive and the Northern Antarctic Peninsula region is very difficult to access. Indeed, only one mass-balance investigation has been published for the study area (Skvarca et al., 2004). However, there are a wide range of remote methods for calculating glacier ELA (e.g., Carrivick and Brewer, 2004). In this study, five different long-term ELA derivation methods were applied (summarised in the Supplement and in Table 4).

3.2 Calculation of glacier change 1988 – 1997 – 2001 – 2009

Assuming no migration of ice divides, and using the datasets named in Table 1 and in the Supplement, the extent and length of each glacier was also mapped for 1988 and 2001. The ice front positions available in the ADD (from Cook et al., 2005) were used to map ice extents in 1997. However, these data were only available for a limited number of tidewater glaciers. These time slices effectively capture the periods before, during and after ice-shelf collapse. The difference in area of each glacier polygon for each time slice allowed calculation of area lost and rates of recession. Annual rates of glacier recession were calculated for each period. In subsequent analyses, glacier surface areas that changed less than the calculated mapping error were classified as "stationary". "Shrinkage" indicates a loss of surface area.

4 2009 Glacier inventory results

4.1 Glacier size and elevation

In 2009, the Northern Antarctic Peninsula region had 194 individual glaciers that covered a total area of $8140 \pm 262\ km^2$ (Fig. 1; Table 5; raw data available for download from GLIMS; www.glims.org). Trinity Peninsula was 95 % glacierised with 62 glaciers covering $5827 \pm 154\ km^2$ (Table 5), which included the largest glaciers on the Northern Antarctic Peninsula with 20 glaciers $> 100\ km^2$. James Ross Island was 75 % glacierised, which is a reduction of 5 % since the survey in 1977 (Rabassa et al., 1982). Our inventory identified 104 glaciers on James Ross Island, whereas the original 1977 survey identified 138. This difference is because of the significantly different approach used to map the glaciers (using ice divides and flow unit boundaries to delimit glacier polygons). Many smaller glaciers or possibly snow patches mapped by Rabassa et al. (1982) are no longer discernible. While we attempted to follow the nomenclature used by Rabassa et al. (1982) as far as possible to facilitate data comparisons, it was not

possible in all cases, either because a glacier was not visible, had retreated and divided into two separate ice masses, or because two or more polygons were merged together in line with the structural glaciological and ice divide mapping. Vega Island was 66 % glacierised with four plateau ice caps with nunataks dissecting catchments into 11 outlet glaciers. A total of 24 glaciers covered $168 \pm 15\,km^2$. Snow Hill Island had one large ice cap covering $326 \pm 3.6\,km^2$, and was 96 % glacierised.

The mean elevation of glaciers was skewed towards glaciers in the 200–300 m a.s.l. bin (Fig. 3a). A small number of glaciers over $100\,km^2$ account for most of the glacierised area (Fig. 3b). As the total area of glaciers in the size class 0.1–0.5 km^2 is only $3\,km^2$, the underestimate of glacierised area caused by having a minimum glacier size of $0.1\,km^2$ is likely to be insignificant and certainly considerably less than $3\,km^2$. H_{MEAN} of glaciers on Trinity Peninsula peaked at 400 m a.s.l., reflecting its high mountain chain. James Ross Island had the highest number of glaciers with mean elevations above 200 m. There was a strong correlation of glacier length and maximum elevation ($r^2 = 0.8$; Fig. 3c), and a rather weaker correlation between log glacier area and elevation ($r^2 = 0.5$; Fig. 3d; Table 3). There is a weak relationship with log glacier area, H_{MEAN} and slope (Fig. 3e,f) and between glacier length and slope (Table 3). In general, longer glaciers had a lower slope, with large low-angled ablation areas.

4.2 Glacier form and classification

Outlet or valley glaciers drain the large plateau ice caps that rest on the Trinity Peninsula mountain chain (Table 6). Almost all the glaciers on Trinity Peninsula calve into the ocean. Of these calving glaciers, 10 had floating and 20 had partially floating termini. James Ross Island had 16 glaciers with floating termini (Fig. 4a), 48 land-terminating glaciers and one lacustrine glacier (GIJR86; Table 6). James Ross Island also had 17 out of the 18 small alpine glaciers, which were mostly cirque or small valley glaciers, and the few glacieret and snowfield remnant glaciers in the study area. The remaining islands were characterised by small ice caps. Snow Hill Island ice cap has extensive floating margins.

4.3 Equilibrium line altitudes

There is a very strong regressionc between ELA_{MEDIAN}, ELA_{AAR} and ELA_{THAR} (Fig. 3h; Tables 3, 4 and 5). However, there is considerable scatter in ELA_{HESS} and ELA_{TSL} and they show no correlation with ELA_{MEDIAN} (Table 5; p values of 0.4 and 0.3, respectively). The large standard error indicates little regional consistency in ELA_{TSL}. Mapping snowlines on Trinity Peninsula is likely to produce substantially different results to other methods, as the strong east-west precipitation gradient on Trinity Peninsula results in snow lines close to sea level on the western coast, and snow lines at 300 to 400 m a.s.l. on the Eastern Peninsula. Strong winds also affect the distribution of snow at the end of the ablation season. In addition, it was difficult to achieve total scene coverage for each year mapped, and there are large gaps in the data. These polar glaciers are characterised by complex accumulation zones with patches of accumulation and ablation separated by areas of superimposed ice (Skvarca et al., 2004), making accurate remote mapping of transient snow lines difficult. Furthermore, mapping of snowlines may occur either just after or just before a snowfall event. As snowfalls occur throughout the summer season in polar regions, this is likely to further skew results. Because of these inherent methodological difficulties, large data gaps, large inter-annual scatter and low correlation, ELA_{TSL} was henceforth excluded from the analysis. ELA_{HESS} was also excluded from further analysis as it is likely to only be applicable to 13 land-terminating glaciers (not being generally applicable to marine-terminating glaciers, glaciers with ice falls, glaciers with complex or compound cirques, or glaciers terminating in steep cliffs; Jiskoot et al., 2009), and there was again large scatter and low correlation (Fig. 3h).

ELA_{MEAN} is therefore the average of ELA_{MEDIAN}, ELA_{AAR} and ELA_{THAR}. However, the calculated ELA_{MEAN} for each glacier must necessarily be treated with caution, as it is entirely derived from the altitudinal range and hypsometric curves of the glaciers, has not been checked against mass-balance data, and does not take into account east-west orographic precipitation and wind variations. Standard deviations range from

< 5 m to > 500 m, illustrating the difficulty in obtaining a meaningful parameter from topographical data alone.

Our topographical ELA predictions can be compared with previous mass balance studies carried out on GIV09, Vega Island (Glaciar Bahia del Diablo; Skvarca et al., 2004). GIV09 was, at time of publication, experiencing a negative mass balance, thinning and frontal retreat. Skvarca et al. (2004) found the equilibrium line of GIV09 difficult to determine, as it had an accumulation area with zones of snow accumulation and ablation, separated by zones of superimposed ice. The altitude of zero mass balance was estimated by Skvarca et al. (2004) to be 400 m a.s.l. This is much higher than our remotely mapped ELA_{MEAN} of 245 ± 92 m a.s.l. It is thus possible that our predicted ELA_{MEAN} is an underestimate, but it is impossible to verify without further spatially-distributed mass-balance data.

Figure 4b shows the distribution of ELA over the study region. The subdued topography on Ulu Peninsula, James Ross Island, results in low ELA_{MEAN} of around 100 m a.s.l. However, the glaciers that have accumulation areas on the Mount Haddington Ice Cap can have ELA_{MEAN} > 800 m a.s.l. ELA_{MEAN} on Trinity Peninsula are generally around 500 to 600 m a.s.l., with the exception of GAP60 and 61, which have ELA_{MEAN} of 1194 ± 727 and 1265 ± 787 m a.s.l., respectively. The range of values may be less for land-terminating simple-basin glaciers, whose size may be more closely determined by climatic factors. For example, GIJR103, a grounded valley glacier with a simple basin, has an ELA_{MEAN} of 87 ± 1 m a.s.l. The range of errors for simple basin glaciers with floating tongues (such as, for example, GIJR64, ELA_{MEAN} 909 ± 432 m a.s.l.) may be because of their large low-lying ablation areas.

4.4 Glacier aspect

Mean glacier aspect is summarised in Fig. 4c,e. There is no correlation with elevation (Fig. 3i; Table 5). The aspect of a glacier controls receipt of solar insolation, as well as influencing the drifting of snow through persistent winds. Most glaciers display asymmetry over their surface area, which results, for example, in a strong northeast to

west-facing preferred glacier aspect on Trinity Peninsula (Fig. 4c). On James Ross Island, there is a preference for northwest-facing aspects. Aspects on Vega Island trend largely southeast and northwest, reflecting the west-east axis of the island.

4.5 Glacier hypsometry

The hypsometric index (HI) of all glaciers was calculated and glaciers were divided into five categories from HI > 1.5 (very bottom heavy) to HI < −1.5 (very top heavy) (Table 7; see Jiskoot et al., 2009). There was considerable inter-catchment variability in glacier shape and elevation distributions. Over half (35) of the large outlet glaciers on Trinity Peninsula were very bottom-heavy, with large low-lying areas below the median altitude (Fig. 4d,f). Exceptions are a few glaciers that terminate within narrow bays (e.g., GAP13, GAP17). However, on the west coast of Trinity Peninsula, glaciers are more equi-dimensional or top-heavy. Glaciers that were formerly tributaries to PGIS were large with relatively small accumulation areas. The remaining glaciers on Eastern Trinity Peninsula were generally bottom-heavy, for example, GAP34, GAP31 and GAP20.

On James Ross Island, the low-lying topography of Ulu Peninsula resulted in bottom-heavy outlet glaciers draining Dobson Dome (Fig. 4d,f), but the large Mount Haddington Ice Cap contained largely top-heavy glaciers, such as GIJR115 and GIJR61. The long-profiles of tidewater outlet glaciers draining the Mount Haddington Ice Cap are typified by sharp changes in slope angle in ice falls at their cirque headwalls, followed by large, low-lying and relatively flat partly floating or floating glacier tongues (Fig. 4g).

In Fig. 5, example normalised hypsometric curves derived from the 2006 SPIRIT DEM are presented and the normalised ELA_{MEAN} has been plotted, which generally fell at about 60 % of the accumulation area. ELA_{MEAN}, which is closely related to median elevation (which was used in the ELA calculation; see Sect. 3.1.5), is a control on glacier recession. The examples in Fig. 5 illustrate the difference between bottom-heavy (GAP12, GAP45), equi-dimensional (GAP14, GAP53) and top-heavy (GAP13, GAP60) glaciers. Glaciers with a small accumulation area could be more sensitive

to climate change if the ELA rises and allows a large additional area to be an ablation zone, especially if the ELA rises above the new median altitude. Comparing the hypsometric curves in Fig. 5 with the long profiles presented in Fig. 4g, it is obvious that the low-lying floating tongues of the Mount Haddington Ice Cap outlet glaciers result in large, low-lying ablation areas that may be vulnerable climate change (rises in temperature or decreases in effective precipitation).

5 Glacier change results

5.1 Change in glacierised area

On Fig. 1, the extent of glaciers in 1988, 1997, 2001 and 2009 is shown, including the former PGIS. For purposes of data summary, where no data are available for a particular year, it is assumed that the area is the same as in the previous analysis from which data is available; however, the values are blank in the figures and Supplement when there is no new data available. The total area given is therefore a minimum value. There was only satellite coverage of all three years (1988, 2001 and 2009) for 178 glaciers. Full rates of glacier recession (with errors) are presented in the Supplement.

In the study region, 90 % of glaciers receded in the period 1988–2001, and 79 % shrank from 2001–2009 (Table 8). On Trinity Peninsula and Vega Islands, advances only occurred from 1988–2001 in two glaciers (GAP10 by $0.73 \pm 0.4\,km^2$; GIV05 by $0.02 \pm 0.01\,km^2$). On James Ross Island, GIJR54 ($0.06 \pm 0.04\,km^2$), GIJR71 ($0.10 \pm 0.05\,km^2$) and GIJR90 ($0.22 \pm 0.2\,km^2$) advanced from 1988–2001. Different glaciers had small advances from 2001–2009 (GIJR124 by $0.46 \pm 0.12\,km^2$; GIJR72 by $1.11 \pm 0.15\,km^2$; and GIJR78 by $0.10 \pm 0.03\,km^2$). It is noteworthy that different glaciers advanced in each time period, and that the number of advancing glaciers has decreased since 2001; this variance highlights the individual dynamics of these glaciers. Most of the advancing glaciers were marine-terminating outlet glaciers, which may have a non-linear response to atmospheric forcing.

The 61 tidewater glaciers and single land-terminating glacier on Trinity Peninsula cover $5827.3 \pm 153.9\,km^2$, and from 1988–2001, lost $727.8\,km^2$, equivalent to an average recession rate of $56\,km^2\,a^{-1}$. These glaciers then retreated at a rate of $16.8\,km^2\,a^{-1}$ in the 8 yr from 2001–2009. The 104 glaciers on James Ross Island lost $290 \pm 15.2\,km^2$ of surface area between 1988 and 2001, and $121.9 \pm 15.2\,km^2$ between 2001 and 2009 (Table 9). This equates to an overall retreat rate on James Ross Island of $22.3\,km^2\,a^{-1}$ over the 13 yr from 1988–2001, and $15.1\,km^2\,a^{-1}$ over the 8 yr from 2001–2009. Two small glaciers (GIJR56 and GIJR30) on James Ross Island disappeared between 1988 and 2009. The majority of the area lost on James Ross Island is accounted for by the disintegration of PGIS in 1995. For most glaciers, the annual rate of retreat has accelerated since 2001, with those on Eastern Antarctic Peninsula and James Ross Island exhibiting particularly rapid recession.

5.2 Land-terminating glaciers

The recession of land-terminating glaciers is of particular interest because their activity is directly related to atmospheric and climatic changes, and these glaciers are scarce on the Antarctic Peninsula (Skvarca and De Angelis, 2003). In the study region, they are generally small; most are less than $1\,km^2$, and so would be expected to react fastest to external forcings (Paul et al., 2004), although this can vary regionally (Raper and Braithewaite, 2009). Response times are also determined by slope and mass balance gradient (Oerlemans, 2005); Fig. 3f illustrates that there is a weak negative relationship between glacier area and mean slope, and that smaller glaciers are often steeper (p value of 0.001).

The seven land-terminating glaciers on Vega Island have all retreated since 1988 (Fig. 6a,b). However, there has been little shrinkage in these glaciers since 2001. Most glacier retreat on Vega Island occurred in the period 1988–2001, with the glaciers generally shrinking by 2 to 7 % (Fig. 6a). The majority of the 48 land-terminating glaciers on James Ross Island are $< 1\,km^2$, but the shrinkage of these glaciers is highly variable. For glaciers $< 1\,km^2$, the percentage shrinkage varies from 0 to 66 %

(Fig. 6c,d). Glaciers $< 3\,km^2$ also show highly variable patterns of shrinkage, from 0 to 35 % (Fig. 7e,f). Overall, the largest reaction to climate warming in the Antarctic Peninsula is in small land-terminating mountain glaciers that are less than $1\,km^2$. Indeed, there is a weak regression between initial glacier size (1988) and total glacier area lost (1988–2009; $r^2 = 0.19$; Fig. 6g; Table 5).

From previous inventories, it is evident that most of the margins land-terminating glaciers in the Northern Antarctic Peninsula region were stationary until 2001–2002, whereupon shrinkage was widely observed (Rau et al., 2004). Our study shows that glacier recession has continued since this period. However, the largest areal changes were observed in the period 1988–2001. Figure 6h shows that the largest annual rates of recession on James Ross Island were between 1988–2001, with only limited recession of land-terminating glaciers after this period. This supports initial observations by Rau et al. (2004). In the period 1975–1988, five land-terminating glaciers were found to be retreating; in the period 1988–2002, 17 out of 21 land-terminating glaciers were retreating. Of the 48 land-terminating glaciers we mapped on the island, 36 out of the 48 mapped land-terminating glaciers had retreated from 1988–2001. In the period 2001–2009, 15 glaciers had retreated. In both time periods, the remaining glaciers were stationary and none had advanced.

5.3 Marine-terminating glaciers

In total, glaciers receded by $1319.5 \pm 395.6\,km^2$ in the Northern Antarctic Peninsula between 1988 and 2009. Of this areal decline, 70 % ($927.7 \pm 395.6\,km^2$) occurred prior to 1997 with the disintegration of PGIS in 1995 (Table 8). However, glacier recession has continued, with $274 \pm 49.1\,km^2$ lost since 2001; this is equivalent to a total recession rate of $30.4 \pm 1.0\,km^2\,a^{-1}$ since 2001 (error estimated probabilistically). On Vega Island, Glaciar Bahia del Diablo (GIV09; Fig. 1) was relatively stable in the period 1982–1985, but showed considerable thinning from 1985–1998, with an average surface lowering of 13.1 m (Skvarca and De Angelis, 2003). Our study of GIV09 from 1988–2009 shows continued shrinkage ($0.5\,km^2$) since 2001.

The highest annual rate of recession was reached in the period 1988–1997, when Sjögren Glacier (GAP12; Fig. 1) receded at $17.7\,km^2\,a^{-1}$. Sjögren Glacier was a major contributor to the ice shelf, and lost $1.2\,km^2\,a^{-1}$ in the period 1997–2001. The annual rate of recession then accelerated, reaching $2.4\,km^2\,a^{-1}$ in the period 2001–2009. GAP15 was also a major contributor to PGIS and receded at a rate of $13.8\,km^2\,a^{-1}$ from 1988 to 1997, $0.6\,km^2\,a^{-1}$ from 1997 to 2001, and $0.3\,km^2\,a^{-1}$ from 2001 to 2009. There is wide variety in rates of glacier recession; GAP05 is the glacier with the highest annual rate of recession that did not feed PGIS. GAP05 lost 9.1 % of its total area in the period 1988–2009, with recession rates of $0.4\,km^2\,a^{-1}$ from 1988 to 2001 and $1.0\,km^2\,a^{-1}$ from 2001 to 2009. The glaciers of Western Trinity Peninsula have had very low rates of recession or have remained stationary.

The recession of glaciers (decrease in glacier length) was greatest for ice-shelf tributary glaciers. For example, Sjögren Glacier (GAP12) retreated 33 km from 1988 to 2001 and 7.1 km from 2001 to 2009 (Fig. 7a), and GAP01 to GAP14 had faster annual rates of glacier retreat both from 1988–2001 and 2001–2009. The change in length for non-ice-shelf tributary glaciers is small by comparison, but they generally had faster rates of retreat after 2001. Figure 7c,d shows little correlation between 2009 glacier length, width of calving tongue and rates of glacier retreat (cf. Table 3), but emphasise that rates of length change were faster 1988–2001. Even after 2001, the fastest annual rates of length change are in former PGIS tributary glaciers (Fig. 7b). Glaciers on Western Trinity Peninsula in general show less change in glacier length and area.

Analysing the rates of recession for the glaciers that fed PGIS in more detail, Fig. 7c highlights the difference in GAP15, GAP14 and GAP12. It is apparent that most of the shrinkage of these three glaciers occurred before 1997, immediately preceding ice-shelf disintegration, with slower and steadier retreat thereafter. These areal losses are substantially larger than the mapped errors. The recession rate decreases after this, with less areal loss. On the other hand, for glaciers on James Ross Island, in particular GIJR92 and GIJR90, which are situated in Röhss Bay, the recession rate is fastest after 2001 (Fig. 7c).

5.4 Spatial and temporal patterns of glacier change

On Trinity Peninsula, ice-shelf tributary glaciers retreated fastest overall and particularly rapidly from 1988–2001 (Fig. 8). Regions of exceptionally rapid glacier recession on Trinity Peninsula include Larsen Inlet, Sjögren Inlet, Eyrie Bay and Duse Bay. Almost all glaciers show signs of glacier recession; four glaciers on Trinity Peninsula advanced from 1988–2001 (Table 8), but after 2001 none have advanced more than the error margin. All advances were small and were subsumed by the overall recession from 1988 to 2009. There are fewer data available for Western Antarctic Peninsula, but shrinkage rates for the period 1988–2009 have remained low in that region (Fig. 9). This contrasts with glaciers on North-Eastern Trinity Peninsula (Fig. 8a).

Some ice-shelf tributary glaciers on James Ross Island also show small signs of advance during the period (Table 8). The remaining glaciers of Röhss Bay experienced enhanced drawdown and faster rates of annual recession after 2001. GIJR90 declined in area at a rate of $1.9\,km^2\,a^{-1}$ from 2001–2009, when the ice shelf retreated beyond the narrow pinning point at the head of Röhss Bay, but the margin was stationary from 1988–2001. This is highlighted in Fig. 8d, which shows the difference in recession between 1988–2001 and 2001–2009. These tidewater glaciers now no longer terminate in a discernible ice shelf, but calve directly into Röhss Bay.

Many large tidewater glaciers on James Ross Island suffered rapid areal decline from 1988 to 2009 (e.g., GIJR108 [$0.6\,km^2\,a^{-1}$], GIJR115 [$0.5\,km^2\,a^{-1}$], and GIJR128 [$0.4\,km^2\,a^{-1}$] (Fig. 1)). There is strongly asynchronous behaviour (Fig. 8a). The glaciers of Croft Bay and GIJR72 [$0.1\,km^2\,a^{-1}$], in Holluschickie Bay, for example, declined comparatively little. Variable rates of areal shrinkage are also noticeable around Cape Broms of Southeast James Ross Island. In general, most glaciers retreated faster from 1988–2001, with some exceptions around Röhss Bay on James Ross Island, Snow Hill Island and the Western Trinity Peninsula (Figs. 7 and 8d, Table 8).

6 Discussion

6.1 Comparison with previous inventories

Our data support the general recessional trend reported in previous inventories (Rabassa et al., 1982; Skvarca et al., 1995; Rau et al., 2004). Our inventory shows a continued and steadily increasing glacier recession since the first inventory 1977 (cf., Rabassa et al., 1982). Average retreat rates for James Ross Island were $1.8\,km^2\,a^{-1}$ in the period 1975–1988, and $2.1\,km^2\,a^{-1}$ in the period 1988–1993 (Skvarca et al., 1995; Rau et al., 2004). Our study indicates that glaciers on James Ross Island retreated at a rate of $22.3\,km^2\,a^{-1}$ from 1988–2001, and $15.1\,km^2\,a^{-1}$ from 2001–2009, indicating increased rates of recession immediately post ice-shelf disappearance but slower rates in the longer-term, which are presumably in response to continued atmospheric and sea surface temperature increases. Given the hypsometry of the large tidewater glaciers draining the Mount Haddington Ice Cap on James Ross Island, these retreat rates are likely to continue if atmospheric temperatures continue to rise.

Overall, recession rates across the Antarctic Peninsula are slowing, which may be as a result of tidewater glaciers reaching their grounding lines, and achieving increased frontal stability. In addition, reported mean annual air temperatures on Ulu Peninsula, James Ross Island, were −5 °C from 1999 to 2004 (Sone et al., 2007) and −7.2 °C from 2006 to 2009 (Laska et al., 2010), suggesting that a few particularly warm years may have made a large difference to overall recession rates. Differences in inter-catchment recession rates may reflect variance in altitude, accumulation area, shifting ice divides, and non-linear tidewater glacier responses to oceanic and atmospheric forcing.

6.2 Impact of the disintegration of Prince Gustav Ice Shelf

The remnant of PGIS in Röhss Bay on James Ross Island (Fig. 1) dramatically disintegrated after 2001. Small ice shelves are susceptible to small changes in temperature and mass balance of tributary glaciers (Glasser et al., 2011). The retreat of ice

shelves from pinning points (such as Persson Island) can result in enhanced calving and rapid retreat. The acceleration of recession of the ice shelf in Röhss Bay after 2001 was therefore caused by ice-dynamical factors, exacerbated by continued atmospheric warming. Small amounts of growth in some ice-shelf glaciers was observed from 1988 to 2001, which could be because of pinning against Persson Island and the mainland of James Ross Island, and structural and dynamic variations in ice-shelf configuration. However, this advance was subsumed by the overall large glacier shrinkage (cf. Fig. 8). In addition, up-glacier thinning may result in steepening, increased driving stress, faster flow, and short-term advance (cf., Meier and Post, 1987).

The recession of marine-terminating glaciers in the Northern Antarctic Peninsula highlights some important trends. For glaciers feeding PGIS, rates of recession were highest during the period of ice-shelf disintegration. Ice-shelf removal can lead to the destabilisation of tributary glaciers, as ice shelves reduce longitudinal stresses and limit glacier motion upstream of the ice shelf (Rignot et al., 2004; Pritchard and Vaughan, 2007; Hulbe et al., 2008). These tributary glaciers began to stabilise and reach a new dynamic equilibrium after 2001 and rates of recession began to reduce once they become stabilised in their narrow fjords. Indeed, fjord geometry has previously been observed to be a major control on tidewater glacier advance and recession rates (Meier and Post, 1987). After 2001, the region therefore entered a period of "normal" glacier recession. The Northern Antarctic Peninsula region has thus had three distinctive phases: 1988–1995, the stable ice-shelf period; 1995–2001, the period of ice-shelf disintegration and rapid readjustment of the ice-shelf tributary glaciers to new boundary conditions; and 2001–2009, when all glaciers are retreating in response to changes in atmospheric and oceanic temperatures. The more rapid recession of the ice-shelf tributary glaciers in Röhss Bay since 2001 (Fig. 8c) is a response to the initial pinning of the ice-shelf post-break up in the mouth of Röhss Bay. Structural glaciological controls are therefore strongly influencing the patterns and rates of retreat of floating tongues following ice-shelf disintegration. Ice-margins stabilised after 2001 once the glaciers retreated to within their bays with shrinkage slowed as a result of

enhanced back-stress and pinning against the fjord sides.

The majority of the glacier ice lost on James Ross Island is accounted for by the disintegration of PGIS in 1995. For most remaining glaciers, recession rates were highest prior to 2001, with ice-shelf tributary glaciers on Eastern Trinity Peninsula exhibiting particularly rapid recession. Western Trinity Peninsula glaciers had very low rates of recession or have remained unchanged. This differing regional response can probably be attributed to precipitation gradients, exacerbated by climatic warming and differential wind patterns (cf., van Lipzig et al., 2004). As south-westerly winds blow across the Antarctic Peninsula mountains, rising air precipitates moisture as snow in the west, starving the east of precipitation (Aristarain et al., 1987; Vaughan et al., 2003). James Ross Island lies in the precipitation shadow of the Antarctic Peninsula. Higher air temperatures will have resulted in a rise in ELA; smaller accumulation areas mean that glaciers are less able to withstand precipitation starvation.

Previous workers have hypothesised that the disintegration of the ice shelf may have affected the regional climate (Rau et al., 2004). The response of land-terminating glaciers is particularly interesting, because on James Ross Island, these glaciers exhibited their highest annual rates of retreat in the ice-shelf disintegration period. Land-terminating glaciers are directly influenced by climatic perturbations and their mass balances are therefore a sensitive indicator of climate variability (Oerlemans, 2005). It therefore appears that the removal of the ice shelf changed the local climate and thus had a strong impact on the island's glaciers. It has been suggested that ice-shelf break up would immediately affect the climate system through the formation of deep water (Hulbe et al., 2004). The removal of the ice shelf would have raised local air temperatures through the availability of more ice-free water in summer. In addition, small glaciers on James Ross Island may be particularly susceptible to changes in local climate because of the large land area, which has a low albedo.

6.3 Glacier hypsometry

Topography and hypsometry are important factors in influencing glacier mass balance, and may explain some of the inter-catchment variability in recession rates. Figure 8c shows GAP17 and GAP18 (both outlet tidewater glaciers) receding at different rates. GAP17 remained stationary during the period 2001–2009, whilst the adjacent GAP18 retreated at $0.2 \pm 0.6\,km^2\,a^{-1}$ during the same interval. However, GAP17 has a very top-heavy HI index of −1.6, compared with 1.8 for GAP18 (cf. Fig. 5d). The more stable glaciers on the Western Peninsula typically have equi-dimensional or top-heavy hypsometric curves (Figs. 4 and 5), which combined with high snowfalls (van Lipzig et al., 2004), render them less susceptible to the changes in ELA brought about by changing atmospheric temperatures (cf., Jiskoot et al., 2009). These glaciers have accumulation areas situated at high altitudes, which contributes to their stability. The hypsometric curves of these grounded tidewater glaciers indicate that they will retain large accumulation areas if future recession occurs and thus recession will be slow, rendering them less sensitive to an upwards shift in the ELA.

The outlet glaciers draining Mount Haddington Ice Cap typically have a large upland accumulation area on the ice cap, a steep icefall over cirque headwalls, and a very flat and low-lying partly floating or floating tongue. These attributes can be observed in the stepped hypsometric curves of GIJR123 and GIJR115 (Fig. 6). This unusual glacier long profile (Fig. 4g) is bedrock-controlled. Vertical joints in the hard Neogene basalts and hyaloclastites encourage the formation of steep cirque headwalls. The glaciers then erode a deep basin in the softer Cretaceous sandstone and mudstone beneath, resulting in partly floating to floating glacier tongues. Rising sea levels would encourage further grounding-line retreat.

6.4 Changes in equilibrium line altitude

If atmospheric temperature rises over the Antarctic Peninsula continue at the current rate of 2.5 °C per 50 yr (Vaughan et al., 2003; IPCC, 2007), a rise of 2 °C could be

reached in the Antarctic Peninsula region between the "present" and the year 2040. Given a calculated adiabatic lapse rate of −5.8 °C per 1000 m (Aristarain et al., 1987), and assuming that the topographic ELA values calculated are representative of the current isoline of zero mass balance on these glaciers, an increase of 2 °C would raise ELAs over the Northern Antarctic Peninsula by 345 m. This is illustrated as ELA_{2C} on the hypsometric curves in Fig. 5, and it is immediately obvious that the differential hypsometry of the glaciers may be an important control on rates of recession in the future. Bottom-heavy glaciers with low-lying ELA_{MEAN} values (such as GAP12) and top-heavy glaciers with high ELA_{MEAN} values (such as GAP13; Fig. 5) are most sensitive to change. In general, however, the tidewater glaciers on Eastern Trinity Peninsula have large, high-elevation accumulation areas. Without a further strong perturbation to the prevailing climate, these large tidewater glaciers will most likely stabilise when they reach their grounding-lines. The ELA_{2C} calculated for these glaciers (Fig. 5) indicates that even with a 2 °C rise in temperature, glaciers will still retain accumulation areas covering at least 40 % of the glacier surface, assuming that glacier hypsometries remain similar. The steady steep slopes on these glaciers also render them less vulnerable; a rise in ELA does not expose a significantly larger area to ablation. Additionally, as these glaciers retreat towards the grounding-line zones, ablation areas will decrease in size, resulting in a more stable mass balance.

The tidewater glaciers on James Ross Island are likely to be extremely vulnerable to a 345 m rise in ELA. GIJR27, for example, may be particularly vulnerable as this tidewater glacier has a large, low-lying flat tongue, and ELA_{2C} plots above the accumulation area. Other glaciers with low-lying tongues will have projected accumulation areas covering only 20–30 % of their area (e.g., GIJR72, GIJR115, GIJR128, GIJR136). These glaciers are likely to continue to retreat very rapidly. Furthermore, the large accumulation areas of glaciers on Mount Haddington Ice Cap are fairly flat. An increase in ELA will result in rapid loss of accumulation area here.

6.5 Oceanic temperatures and climate forcing

The calving flux and recession of tidewater glaciers in the study region is likely to be largely controlled by non-linear glacier responses to changes in oceanic temperatures as well as atmospheric temperature and precipitation gradients. Ocean temperatures around the Western Antarctic Peninsula have risen by more than 1 °C since 1951 (Gille, 2002, 2008; Meredith and King, 2005), driven by reduced sea-ice formation and atmospheric warming. Changes in sea-surface temperatures (and sea ice extent) may influence enhance bottom melting and thinning (Holland et al., 2010) and therefore propensity to calve (Benn et al., 2007a), thus accelerating terminus retreat. Tensile strength of glacier ice decreases as ice becomes more temperate, resulting in increased calving rates (Powell, 1991). Furthermore, retreat of the terminus, as a result of increased calving, leads to larger up-glacier stretching rates, greater ice speeds and glacier thinning, further exacerbating increased calving rates for tidewater glaciers (Meier and Post, 1987; van der Veen, 2002), and possibly contributing to short-term small glacier advances.

The observed asymmetry and variability in recession in tidewater glaciers may be explained by complex calving processes. The calving flux of tidewater glaciers is controlled by crevasse depth, ice velocity, strain rates, ice thickness and water depth (Benn et al., 2007a). In grounded tidewater glaciers, terminus position may be controlled by the local geometry of the fjord (van der Veen, 2002). Rapid recession of tidewater glaciers in the region is likely to be enhanced by the asymmetry of the calving flux between advancing and retreating glaciers, with increased calving exacerbating the recessional trends (Benn et al., 2007b).

7 Conclusions

The Antarctic Peninsula is experiencing rapid atmospheric warming, which has resulted in the disintegration of many ice shelves (Scambos et al., 2003; Hulbe et al.,

2008; Glasser and Scambos, 2008; Cook and Vaughan, 2010). Numerous papers have documented the disintegration of those ice shelves, but this is the first to thoroughly and quantitatively investigate changes in all glaciers in the Trinity Peninsula region. We provide the first detailed inventory of 194 glaciers on Trinity Peninsula and islands to the southeast, with detailed estimates of size, length, elevation ranges, ELA, slope, aspect, hypsometry, morphological descriptors, form and classification. These data will be invaluable to numerical modellers seeking to predict the future behaviour of this climatically sensitive region. The full glacier inventory is available for download from GLIMS (www.glims.org).

We measured variability in glacier length and area changes on the Northern Antarctic Peninsula between 1988, 1997, 2001 and 2009. This inventory provides important data for monitoring glacier recession on the Antarctic Peninsula. Changes in glacier area and length presented in this tudy considerably extend the hitherto available geographical coverage and amount of detail available for understanding the impacts of climate change on the cryosphere.

Of the 194 glaciers surveyed, 90 % showed rapid retreat from 1988–2001 and 79 % retreated from 2001–2009, although the rates and patterns of recession vary substantially. Overall, annual rates of recession were higher from 1988–2001 in tidewater and ice-shelf tributary glaciers. Some glaciers on Western Trinity Peninsula, glaciers in Röhss Bay on James Ross Island and Snow Hill Island retreated faster from 2001–2009. Annual rates of recession in land-terminating glaciers were also higher from 1988–2001. Three distinct phases were observed: 1988–1997 (the ice-shelf and ice-shelf disintegration era); 1997–2001 (period of immediate adjustment); 2001–2009 (period of stabilisation and long-term adjustment to new dynamic equilibrium and general climate-driven recession). Total glacierised area in the Northern Antarctic Peninsula has declined at an average of $30.4 \pm 0.99\,\mathrm{km^2\,a^{-1}}$ since 2001 (error estimated probabilistically), with total losses of glacierised area of 11.1 % from 1988–2001 and 3.3 % from 2001–2009.

Tidewater glaciers on Western Trinity Peninsula remained stable between 1988 and 2009, and to date show only slow rates of retreat. They receive abundant snow from prevailing south-westerly winds, and, unless strong perturbation to this system occurs, will probably remain stable in areal extent. This inference does not take account of glacier thinning, which is observed in other parts of the Antarctic Peninsula, even after frontal stabilisation has occurred (Rott et al., 2011). In contrast, large tidewater glaciers on the Eastern Trinity Peninsula are apparently more vulnerable to continued climate warming, but they may stabilise in the future as they retreat towards their grounding zones.

Glaciers on Trinity Peninsula that fed PGIS have stabilised since 2001, with slower annual recession rates since then. On James Ross Island, the largest areal changes have been from low-lying tidewater glaciers. Annual tidewater glaciers recession rates are likely to continue in response to continued atmospheric warming. The primary control for the widespread glacier retreat in Northeast Antarctic Peninsula is apparently the observed climatic warming, with glacier size, length, slope, type, ELA and altitude exerting a strong mitigating or enhancing role.

Despite fears of continued run-away retreat and terminal destabilisation of tidewater glaciers, this study shows that ice-shelf tributary glaciers are more likely to undergo a time-limited period of adjustment. Ultimately, ice-shelf tributary glaciers will find a new dynamic equilibrium, and then retreat slowly in response to warming climates and rising ELAs. We therefore anticipate that the results of this project will be relevant to studies concerned with the more southerly ice shelves that surround the Antarctic Peninsula. The behaviour of PGIS tributary glaciers and their long-term response to ice-shelf removal can be used to model and predict glacier response to contemporary and future ice-shelf disintegration events.

Supplementary material related to this article is available online at: http://www.the-cryosphere-discuss.net/5/3541/2011/tcd-5-3541-2011-supplement.zip

Supplementary Methods. Detailed information on methods used in glacier attribute data acquisition.

Supplementary Data. Dataset for the analysis of glacier change, with areas, lengths, and errors for 1988, 1997, 2001 and 2009. Also given are calculated rates of change and the difference in rates of recession. Raw data and shapefiles are available from GLIMS (www.glims.org).

Acknowledgements. This work was funded by NERC grant AFI 9-01 (NE/F012942/1). It is a contribution to the SCAR ACE (Antarctic Climate Evolution) Programme. The authors are grateful for helpful and constructive criticism and comments from Hester Jiskoot and Tobias Bolch. The authors acknowledge Etienne Berthier and the Centre National d'Etudes Spatiales (CNES) for the SPOT-5 images and the SPIRIT DEM. Neil Glasser was provided with no-cost access to ASTER images from NASA as a NASA-supported researcher. The 1997 glacier frontal positions were determined from the ADD (http://www.add.scar.org:8080/add/) Coastal Change shapefiles, mapped by Cook et al. (2005). Stefan Senk and Tristram Irvine-Fynne are acknowledged for their help in programming and statistical analysis.

References

Abermann, J., Lambrecht, A., Fischer, A., and Kuhn, M.: Quantifying changes and trends in glacier area and volume in the Austrian Ötztal Alps (1969–1997–2006), The Cryosphere, 3, 205–215, doi:10.5194/tc-3-205-2009, 2009. 3543

Aristarain, A. J., Pinglot, J. F., and Pourchet, M.: Accumulation and temperature measurements on the James Ross Island ice cap, Antarctic Peninsula, Antarctica, J. Glaciol., 33, 357–362, 1987. 3564, 3566

Benn, D. I., Hulton, N. R. J., and Mottram, R. H.: "Calving laws", "sliding laws" and the stability of tidewater glaciers, Ann. Glaciol., 46, 123–130, 2007a. 3567

Benn, D. I., Warren, C. R., and Mottram, R. H.: Calving processes and the dynamics of calving glaciers, Earth-Sci. Rev., 82, 143–179, 2007b. 3567

Berthier, E., Arnaud, Y., Kumar, R., Ahmad, S., Wagnon, P., and Chevallier, P.: Remote sensing estimates of glacier mass balances in the Himachal Pradesh (Western Himalaya, India), Remote Sens. Environ., 108, 327–338, 2007. 3548

Bolch, T., Menounos, B., and Wheate, R.: Landsat-based inventory of glaciers in Western Canada, 1985–2005, Remote Sens. Environ., 114, 127–137, 2010. 3549, 3579
Braithwaite, R. J. and Raper, S. C. B.: Estimating equilibrium-line altitude (ELA) from glacier inventory data, Ann. Glaciol., 50, 127–132, 2009. 3551
British Antarctic Survey: James Ross Island, BAS 100 Series (topographic maps), Sheet 2, 1 : 100000, British Antarctic Survey, Cambridge, 1995. 3548
British Antarctic Survey: Antarctic Sound and James Ross Island, Northern Antarctic Peninsula, Series BAS (UKAHT) Sheets 3A and 3B, 1 : 250000, Cambridge, United Kingdom Antarctic Heritage Trust, 2010. 3548
Brunt, K. M., Fricker, H. A., Padman, L., Scambos, T. A., and O'Neel, S.: Mapping the grounding zone of the Ross Ice Shelf, Antarctica, using ICESat laser altimetry, Ann. Glaciol., 51, 71–79, 2010. 3550
Carrivick, J. L. and Brewer, T. R.: Improving local estimations and regional trends of glacier equilibrium line altitudes, Geogr. Ann. A, 86, 67–79, 2004. 3551
Carrivick, J. L. and Chase, S. E.: Spatial and temporal variability in the net mass balance of glaciers in the Southern Alps, New Zealand, New Zeal. J. Geol. Geop., 54, 415–429, 2011. 3551
Carrivick, J. L., Davies, B. J., Glasser, N. F., and Nyvlt, D.: Late Holocene changes in character and behaviour of land-terminating glaciers on James Ross Island, Antarctica, J. Glaciol., submitted, 2011. 3550
Cook, A. J. and Vaughan, D. G.: Overview of areal changes of the ice shelves on the Antarctic Peninsula over the past 50 years, The Cryosphere, 4, 77–98, doi:10.5194/tc-4-77-2010, 2010. 3543, 3547, 3568
Cook, A. J., Fox, A. J., Vaughan, D. G., and Ferrigno, J. G.: Retreating glacier fronts on the Antarctic Peninsula over the past half-century, Science, 308, 541–544, 2005. 3543, 3548, 3552, 3570
Cooper, A. P. R.: Historical observations of Prince Gustav Ice Shelf, Polar Rec., 33, 285–294, 1997. 3547
Czech Geological Survey: James Ross Island – Northern Part, Topographic Map 1 : 25000, Czech Geological Survey, Praha, 2009. 3548
Dahl, S. O. and Nesje, A.: Paleoclimatic implications based on equilibrium-line altitude depressions of reconstructed Younger Dryas and Holocene cirque glaciers in inner Nordfjord, western Norway, Palaeogeogr. Palaeocl., 94, 87–97, 1992. 3550

De Angelis, H. and Skvarca, P.: Glacier surge after ice shelf collapse, Science, 299, 1560–1562, 2003. 3543
Evans, J., Pudsey, C. J., Ó Cofaigh, C., Morris, P., and Domack, E.: Late Quaternary glacial history, flow dynamics and sedimentation along the eastern margin of the Antarctic Peninsula Ice Sheet, Quaternary Sci. Rev., 24, 741–774, 2005.
Ferrigno, J. G., Cook, A. J., Foley, K. M., Williams, R. S., Swithinbank, C., Fox, A. J., Thomson, J. W., and Sievers, J.: Coastal-Change and Glaciological Map of the Trinity Peninsula Area and South Shetland Islands, Antarctica: 1843–2001, USGS, 32 pp., Denver, 2006. 3546, 3547
Fricker, H. A., Coleman, R., Padman, L., Scambos, T. A., Bohlander, J., and Brunt, K. M.: Mapping the grounding zone of the Amery Ice Shelf, East Antarctica using InSAR, MODIS and ICESat, Antarct. Sci., 21, 515–532, 2009. 3550
Fukuda, M., Strelin, J. A., Shimokawa, K., Takahashi, N., Sone, T., and Trombott, D.: Permafrost occurrence of Seymour Island and James Ross Island, in: Recent Progress in Antarctic Earth Science, edited by: Yoshida, Y., Kaminuma, K., and Shiraishi, K., Terra Science Publishers, Tokyo, 745–750, 1992. 3546
Furbish, D. J. and Andrews, J. T.: The use of hypsometry to indicate long-term stability and response of valley glaciers to changes in mass transfer, J. Glaciol., 30, 199–211, 1984. 3551
Gille, S. T.: Warming of the Southern Ocean since the 1950s, Science, 295, 1275–1277, 2002. 3567
Gille, S. T.: Decadal-scale temperature trends in the Southern Hemisphere Ocean, J. Climatol., 21, 4749–4765, 2008. 3546, 3567
Glasser, N. F. and Scambos, T. A.: A structural glaciological analysis of the 2002 Larsen B Ice Shelf collapse, J. Glaciol., 54, 3–16, 2008. 3568
Glasser, N. F., Kulessa, B., Luckman, A., Jansen, D., King, E. C., Sammonds, P. R., Scambos, T. A., and Jezek, K. C.: Surface structure and stability of the Larsen C Ice Shelf, Antarctic Peninsula, J. Glaciol., 55, 400–410, 2009.
Glasser, N. F., Scambos, T. A., Bohlander, J. A., Truffer, M., Pettit, E. C., and Davies, B. J.: From ice-shelf tributary to tidewater glacier: continued rapid glacier recession, acceleration and thinning of Röhss Glacier following the 1995 collapse of the Prince Gustav Ice Shelf on the Antarctic Peninsula, J. Glaciol., 57, 397–406, 2011. 3544, 3547, 3562
Granshaw, F. D. and Fountain, A. G.: Glacier change (1958–1998) in the North Cascades National Park Complex, Washington, USA, J. Glaciol., 52, 251–256, 2006. 3548, 3579

Hambrey, M. J., Smellie, J. L., Nelson, A., and Johnson, J. S.: Late Cenozoic glacier-volcano interaction on James Ross Island and adjacent areas, Antarctic Peninsula, Geol. Soc. Am. Bull., 120, 709–731, 2008. 3546

Heroy, D. C. and Anderson, J. B.: Ice-sheet extent of the Antarctic Peninsula region during the Last Glacial Maximum (LGM) – insights from glacial geomorphology, Geol. Soc. Am. Bull., 117, 1497–1512, 2005. 3546

Hock, R., de Woul, M., Radic, V., and Dyurgerov, M.: Mountain glaciers and ice caps around Antarctica make a large sea-level rise contribution, Geophys. Res. Lett., 36, 1–5, 2009. 3543

Holland, P. R., Jenkins, A., and Holland, D. M.: Ice and ocean processes in the Bellingshausen Sea, Antarctica, J. Geophys. Res., 115, C05020, doi:10.1029/2008/JC005219, 2010. 3567

Hulbe, C. L., MacAyeal, D. R., Denton, G. H., Kleman, J., and Lowell, T. V.: Catastrophic ice shelf break up as the source of Heinrich Event icebergs, Paleoceanography 19, PA1004, doi:10.1029/2003pa000890, 2004. 3564

Hulbe, C. L., Scambos, T. A., Youngberg, T., and Lamb, A. K.: Patterns of glacier response to disintegration of the Larsen B ice shelf, Antarctic Peninsula, Global Planet. Change, 63, 1–8, 2008. 3563, 3567

IPCC: IPCC Fourth Assessment Report: Climate Change 2007, Cambridge University Press, Cambridge, 2007. 3565

Jiskoot, H., Murray, T., and Boyle, P.: Controls on the distribution of surge-type glaciers in Svalbard, J. Glaciol., 46, 412–422, 2000.

Jiskoot, H., Curran, C. J., Tessler, D. L., and Shenton, L. R.: Changes in Clemenceau Icefield and Chaba Group glaciers, Canada, related to hypsometry, tributary detachment, length-slope and area-aspect relations, Ann. Glaciol., 50, 133–143, 2009. 3551, 3554, 3556, 3565, 3584

King, J. C.: Recent climate variability in the vicinity of the Antarctic Peninsula, Int. J. Climatol., 14, 357–369, 1994. 3543

King, J. C., Turner, J., Marshall, G. J., Connelly, W. M., and Lachlan-Cope, T. A.: Antarctic Peninsula climate variability and its causes as revealed by analysis of instrumental records, in: Antarctic Peninsula Climate Variability: Historical and Palaeoenvironmental Perspectives, edited by: Domack, E. W., Leventer, A., Burnett, A., Bindschadler, R., Convey, P., and Kirby, M.: Antarctic Research Series, American Geophysical Union, Washington, D.C., 17–30, 2003. 3545

Korona, J., Berthier, E., Bernard, M., Remy, F., and Thouvenot, E.: SPIRIT, SPOT 5 stereo-

scopic survey of Polar Ice: reference images and topographies during the fourth International Polar Year (2007–2009), Int. Soc. Photogramme., 64, 204–212, 2009. 3548

Lambrecht, A., Sandhager, H., Vaughan, D. G., and Mayer, C.: New ice thickness maps of Filchner-Ronne Ice Shelf, Antarctica, with specific focus on grounding lines and marine ice, Antarct. Sci., 19, 521–532, 2007. 3550

Laska, K., Prosek, P., and Budik, L.: Seasonal variation of air temperature at the Mendel Station, James Ross Island, in the period of 2006–2009, Geophysical Research Abstracts 12, EGU2010-3880, 2010. 3562

Leclercq, P. W., Oerlemans, J., and Cogley, J. G.: Estimating the glacier contribution to sea-level rise for the period 1800–2005, Surv. Geophys., 32, 1–17, doi:10.1007/s10712-011-9121-7, 2011. 3543

van Lipzig, N. P. M., King, J. C., Lachlan-Cope, T., and van den Broeke, M.: Precipitation, sublimation and snow drift in the Antarctic Peninsula region from a regional atmospheric model, J. Geophys. Res., 109, D24106, 1–16, 2004. 3546, 3564, 3565

Lopez, P., Chevallier, P., Favier, V., Pouyaud, B., Ordenes, F., and Oerlemans, J.: A regional view of fluctuations in glacier length in southern South America, Global Planet. Change, 71, 85–108, 2010.

Martin, P. J. and Peel, D. A.: The spatial distribution of 10 m temperatures in the Antarctic Peninsula, J. Glaciol., 20, 311–317, 1978. 3545

Mayewski, P. A., Meredith, M. P., Summerhayes, C. P., Turner, J., Worby, A., Barrett, P. J., Casassa, G., Bertler, N. A. N., Bracegirdle, T., Naveira Garabato, A. C., Bromwich, D., Campell, H., Hamilton, G. S., Lyons, W. B., Maasch, K. A., Aoki, S., Xiao, C., and van Ommen, T.: State of the Antarctic and Southern Ocean climate system, Rev. Geophys., 47, 1–38, 2009. 3546

Meier, M. F. and Post, A.: Fast tidewater glaciers, J. Geophys. Res., 92, 9051–9058, 1987. 3563, 3567

Meredith, M. P. and King, J. C.: Rapid climate change in the ocean west of the Antarctic Peninsula during the second half of the 20th Century, Geophys. Res. Lett., 32, doi:10.1029/2005GL024042, 2005. 3567

Morris, E. M. and Vaughan, A. P. M.: Spatial and temporal variation of surface temperature on the Antarctic Peninsula and the limit of viability of ice shelves, in: Antarctic Peninsula Climate Variability: Historical and Palaeoenvironmental Perspectives, edited by: Domack, E. W., Leventer, A., Burnett, A., Bindschadler, R., Convey, P., and Kirby, M.: Antarctic Research Series,

American Geophysical Union, Washington, D.C., Vol. 79, 61–68, 2003. 3543
Oerlemans, J.: Extracting a climate signal from 169 glacier records, Science, 308, 675–677, 2005. 3550, 3558, 3564
Osmaston, H.: Estimates of glacier equilibrium line altitudes by the Area x Altitude, the Area x Altitude Balance Ratio and the Area x Altitude Balance Index methods and their validation, Quaternary International 138–139, 22–31, 2005.
Paul, F. and Svoboda, F.: A new glacier inventory on Southern Baffin Island, Canada, from ASTER data: II. Data analysis, glacier change and applications, Ann. Glaciol., 50, 22–31, 2009.
Paul, F., Kääb, A., Maisch, M., Kellenberger, T., and Haeberli, W.: Rapid disintegration of Alpine glaciers observed with satellite data, Geophys. Res. Lett., 31, L21402, doi:10.1029/2004GL020816, 2004. 3558
Paul, F., Barry, R. G., Cogley, J. G., Frey, H., Haeberli, W., Ohmura, A., Ommanney, C. S. L., Raup, B., Rivera, A., and Zemp, M.: Guidelines for the compliation of glacier inventory data from digital sources, GLIMS, Global Land Ice Measurement from Space, NSIDC, University of Colorado, Boulder, 23 pp., 2010. 3549, 3550
Powell, R. D.: Grounding-line systems as second-order controls on fluctuations of tidewater termini of temperate glaciers, in: Glacial Marine Sedimentation; Palaeoclimatic Significance, Geological Society of America Special Paper 261, edited by: Anderson, J. B. and Ashley, G. M., Boulder, Colorado, 75–94, 1991. 3567
Pritchard, H. D. and Vaughan, D. G.: Widespread acceleration of tidewater glaciers on the Antarctic Peninsula, J. Geophys. Res.-Earth, 112, F03S29, 1–10, 2007. 3543, 3563
Rabassa, J., Skvarca, P., Bertani, L., and Mazzoni, E.: Glacier inventory of James Ross and Vega Islands, Antarctic Peninsula, Ann. Glaciol., 3, 260–264, 1982. 3543, 3544, 3546, 3548, 3552, 3562
Racoviteanu, A. E., Paul, F., Raup, B., Khalsa, S. J. S., and Armstrong, R.: Challenges and recommendations in mapping of glacier parameters from space: results of the 2008 Global Land Ice Measurements from Space (GLIMS) workshop, Boulder, Colorado, USA, Ann. Glaciol., 50, 53–69, 2009. 3543, 3544, 3547, 3549
Raper, S. C. B. and Braithwaite, R. J.: Glacier volume response time and its links to climate and topography based on a conceptual model of glacier hypsometry, The Cryosphere, 3, 183–194, doi:10.5194/tc-3-183-2009, 2009. 3558
Rau, F., Mauz, F., de Angelis, H., Ricardo, J., Neto, J. A., Skvarca, P., Vogt, S., Saurer, H., and

Gossmann, H.: Variations of glacier frontal positions on the Northern Antarctic Peninsula, Ann. Glaciol., 39, 525–530, 2004. 3543, 3544, 3547, 3559, 3562, 3564
Rau, F., Mauz, F., Vogt, S., Khalsa, S. J. S., and Raup, B.: Illustrated GLIMS Glacier Classification Manual, Version 1.0. GLIMS Regional Centre, "Antarctic Peninsula", GLIMS (Global Land Ice Measurement from Space), NSIDC, University of Colorado, Boulder, 36 pp., 2005. 3549, 3579
Raup, B. and Khalsa, S. J. S.: GLIMS Analysis Tutorial, GLIMS, Global Land Ice Measurements from Space, NSIDC, University of Colorado, Boulder, 15 pp., 2010. 3549
Raup, B., Kääb, A., Kargel, J. S., Bishop, M. P., Hamilton, G., Lee, E., Paul, F., Rau, F., Soltesz, D., Khalsa, S. J. S., Beedle, M., and, Helm, C.: Remote sensing and GIS technology in the Global Land Ice Measurements from Space (GLIMS) Project, Comput. Geosci., 33, 104–125, 2007a. 3549
Raup, B., Racoviteanu, A., Khalsa, S. J. S., Helm, C., Armstrong, R., and Arnaud, Y.: The GLIMS geospatial glacier database: A new tool for studying glacier change, Global Planet. Change, 56, 101–110, 2007b. 3549
Reinartz, P., Müller, R., Lehner, M., and Schroeder, M.: Accuracy analysis for DEM and orthoimages derived from SPOT HRS stereo data using direct georeferencing, Int. Soc. Photogramme., 60, 160–169, 2006. 3548, 3550
Rignot, E., Casassa, G., Gogineni, P., Krabill, W., Rivera, A., and Thomas, R.: Accelerated ice discharge from the Antarctic Peninsula following the collapse of Larsen B ice shelf, Geophys. Res. Lett., 31, doi:10.1029/2004gl020697, 2004. 3563
Rott, H., Skvarca, P., and Nagler, T.: Rapid collapse of Northern Larsen Ice Shelf, Antarctica, Science, 271, 788–792, 1996. 3544
Rott, H., Müller, F., Nagler, T., and Floricioiu, D.: The imbalance of glaciers after disintegration of Larsen-B ice shelf, Antarctic Peninsula, The Cryosphere, 5, 125–134, doi:10.5194/tc-5-125-2011, 2011.
Scambos, T., Hulbe, C., and Fahnestock, M.: Climate-induced ice shelf disintegration in the Antarctic Peninsula, in: Antarctic Peninsula Climate Variability, edited by: Domack, E. W., Leventer, A., Burnett, A., Bindschadler, R., Convey, P., and Kirby, M.: Antarctic Research Series 79, American Geophysical Union, Washington D.C., 79–92, 2003. 3567
Scambos, T. A., Bohlander, J. A., Shuman, C. A., and Skvarca, P.: Glacier acceleration and thinning after ice shelf collapse in the Larsen B embayment, Antarctica, Geophys. Res. Lett., 31, L18402, doi:10.1029/2004GL020670, 2004. 3543, 3550

Schiefer, E., Menounos, B., and Wheate, R.: An inventory and morphometric analysis of British Columbia glaciers, Canada, J. Glaciol., 54, 551–560, 2008.
Skvarca, P. and De Angelis, H.: Impact assessment of regional climatic warming on glaciers and ice shelves of the Northeastern Antarctic Peninsula, in: Antarctic Peninsula Climate Variability: Historical and Palaeoenvironmental Perspectives, edited by: Domack, E. W., Leventer, A., Burnett, A., Bindschadler, R., Convey, P., and Kirby, M.: Antarctic Research Series, Vol. 79, American Geophysical Union, Washington, D.C., 69–78, 2003. 3547, 3558, 3559
Skvarca, P., Rott, H., and Nagler, T.: Satellite imagery, a base line for glacier variation study on James Ross Island, Antarctica, Ann. Glaciol., 21, 291–296, 1995. 3543, 3544, 3546, 3547, 3562
Skvarca, P., De Angelis, H., and Ermolin, E.: Mass balance of "Glaciar Bahia del Diablo", Vega Island, Antarctic Peninsula, Ann. Glaciol., 39, 209–213, 2004. 3551, 3554, 3555
Smith, R. and Anderson, J. B.: Ice-sheet evolution in James Ross Basin, Weddell Sea margin of the Antarctic Peninsula: the seismic stratigraphic record, Geol. Soc. Am. Bull., 122, 830–842, 2010. 3543
Smellie, J. L., Johnson, J. S., McIntosh, W. C., Esser, R., Gudmundsson, M. T., Hambrey, M. J., and van Wyk de Vries, B.: Six million years of glacial history recorded in volcanic lithofacies of the James Ross Island Volcanic Group, Antarctic Peninsula, Palaeogeogr. Palaeocl., 260, 122–148, 2008. 3546
Sone, T., Fukui, K., Strelin, J. A., Torielli, C. A., and Mori, J. Glacier lake outburst flood on James Ross Island, Antarctic Peninsula region, Pol. Polar Res., 28, 3–12, 2007. 3562
Stastna, V.: Spatio-temporal changes in surface air temperature in the region of the Northern Antarctic Peninsula and South Shetland Islands during 1950–2003, Polar Science, 4, 18–33, 2010. 3545
Svoboda, F. and Paul, F.: A new glacier inventory on southern Baffin Island, Canada, from ASTER data: I. Applied methods, challenges and solutions, Ann. Glaciol., 50, 11–21, 2009. 3549
Turner, J., Colwell, S. R., Marshall, G. J., Lachlan-Cope, T. A., Carelton, A. M., Jones, P. D., Lagun, V., Reid, P. A., and Iagovkina, S.: Antarctic climate change during the last 50 years, Int. J. Climatol., 25, 279–294, 2005. 3543, 3546
Vaughan, D. G. and Doake, C. S. M.: Recent atmospheric warming and retreat of ice shelves on the Antarctic Peninsula, Nature, 379, 328–331, 1996. 3543
Vaughan, D. G., Marshall, G. J., Connelly, W. M., Parkinson, C., Mulvaney, R., Hodgson, D. A.,

King, J. C., Pudsey, C. J., and Turner, J.: Recent rapid regional climate warming on the Antarctic Peninsula, Climatic Change, 60, 243–274, 2003. 3543, 3545, 3547, 3564, 3565
van den Broeke, M. R. and van Lipzig, N. P. M.: Changes in Antarctic temperature, wind and precipitation in response to the Antarctic Oscillation, Ann. Glaciol., 39, 119–126, 2004. 3545, 3546
van der Veen, C. J.: Calving glaciers, Prog. Phys. Geog., 26, 96–122, 2002. 3567

Table 1. Data sources used in Trinity Peninsula glacier inventory.

Notes	Resolution	Date Captured	Data Source
ASTER VNIR (Advanced Spaceborne Thermal Emission and Reflection Radiometer)	15 m	Various dates from 2001 to 2009*	Sensor on the NASA Terra Satellite. Level 1B Multispectral images. Validated radiometric and geometric coefficients applied. Coverage for each scene is 60 × 60 km. Datum: WGS84 Zone 21S
LANDSAT-4 TM	75 m	29 Feb 1988	Panchromatic image. Scene ID: LT4215105160XXX11
		9 Feb 1990	Panchromatic image. Scene ID: LT42161051990040XXX01
SPOT-5 (Satellite Pour l'Observation de la Terre) HRS (High Resolution Sensor) orthoimages	5 m with an absolute horizontal precision of 30 m RMS (Korona et al., 2009)	Antarctic Peninsula: 7 Jan 2006	Captured at an incidence angle of −22.8°, sun azimuth of 55.2°and sun elevation of 40.5°. Panchromatic image. 120 km swath
		James Ross Island: 23 Jan 2006	Captured at an incidence angle of −22°, sun azimuth of 55°and sun elevation of 37°. Panchromatic image. 120 km swath
SPIRIT DEM (SPOT-5 Stereoscopic Survey of Polar Ice: Reference Images and Topographies)	40 m. Absolute horizontal precision of 30 m RMS. Vertical precision ±6 m	Dates as above for the two DEMs	Derived from the above two large footprint (120 km swath) SPOT-5 HRS stereoscopic pairs (Korona et al., 2009)

* Refer to Supplement for further details of ASTER images.

Table 2. Sources of error and error mitigation in defining the area of each glacier polygon.

Sources of errors	Uncertainty	Mitigation
Ice-divide and drainage basin identification	±10 %	Multiple methods used for ice-divide identification (DEM, visual, glaciological interpretations, slope, aspect, automatic hydrology tools)
Identification of glacier boundaries (digital mapping error) on ASTER images	3 pixels (±22.5 m)	Visual checks and buffer width of 22.5 m on either side of glacier polygon
Identification of glacier boundaries (digital mapping error) on LANDSAT image	3 pixels (±112.5)	Visual checks and buffer width of 112.5 m on either side of glacier polygon
Delineation of debris-covered tongues (Bolch et al., 2010)	±0.5 %	Visual checks and buffer width (as above); checking over several images where possible
Scene quality, clouds, seasonal snow, shadows (Bolch et al., 2010)	±4 %	Snow coverage of glacier margins is covered in the *Remarks* column of the database. See also Table 2. Use of multiple images aids the omission of seasonal snow
Error in co-registration and glacier size (Granshaw and Fountain, 2006)	±15 m (RMS) for VNIR (Rau et al., 2005).	Error is less than 3 pixels so is included in the buffer above

Table 3. Methods of ELA calculation. Refer to the Supplement for more information. Altitudes are derived from the 2006 SPIRIT DEM, and these ELAs are therefore approximations for the year 2006.

Method	Description	Notes
ELA_{MEDIAN}	Median Elevation	Represents an accumulation area ratio (AAR) of 50 %. Equivalent to H_{MEDIAN}
ELA_{AAR}	Accumulation Area Ratio	Assumes an AAR of 60 %; derived from hypsometric curves for the 54 tidewater glaciers over 40 km^2
ELA_{THAR}	Toe to Headwall Ratio	Ratio between minimum and maximum glacier altitude
ELA_{HESS}	Hess method	Transition between convex and concave contours
ELA_{TSL}	Transient Snow Lines	Altitude of the snow line at the end of the ablation season
ELA_{MEAN}	Mean ELA	Mean of ELA_{MEDIAN}, ELA_{AAR}, ELA_{THAR}

Table 4. Summary table of the glaciers of the Northern Antarctic Peninsula. Error is determined by applying a 22.5 m buffer to either side of the glacier polygon. TP = Trinity Peninsula. JRI = James Ross Island. VI = Vega Island. IIC = Island Ice Caps.

	Number of Glaciers	Total glacierised area (km^2)	Total land area (km^2)	% Glacierised
TP	62	5827 ± 154	6160	95
JRI	104	1781 ± 86	2378	75
VI	24	168 ± 15	253	66
IIC	4	365 ± 7	407	90
Total	194	8140 ± 262	9198	89

Table 5. Regression table for variables in the inventory. "*n*" is the number of observations. "ltg" means "land-terminating glaciers". *P*-values are calculated at the 95 % confidence level.

Variable A	Variable B	*n*	Adjusted r^2	Standard error	*P* value
Mean Elevation (H_{MEAN})	$Mean_{ECR}$	192	0.82	102.00	< 0.001
Maximum Elevation	Glacier length	174	0.79	3.10	< 0.001
Maximum Elevation	Glacier area	192	0.48	51.22	< 0.001
Mean Elevation	Glacier area	192	0.30	59.57	< 0.001
Mean Slope	Glacier area	192	0.05	69.38	0.001
Mean Slope	Glacier length	174	0.08	3.14	< 0.001
Mean Aspect	Mean Elevation	192	0.02	235.84	0.160
Mean Aspect	Maximum Elevation	192	0.00	106.81	0.814
ELA_{MEDIAN}	ELA_{AAR}	55	0.95	72.21	< 0.001
ELA_{MEDIAN}	ELA_{THAR}	192	0.62	159.30	< 0.001
ELA_{MEDIAN}	ELA_{HESS}	68	0.00	295.50	0.384
ELA_{MEDIAN}	ELA_{TSL}	152	0.00	263.88	0.290
1988 glacier area (ltg)	Total area lost (ltg)	55	0.19	3.24	< 0.001
Width of calving tongue	Total area lost	115	0.03	8.377	0.041
ELA_{MEAN}	Total area lost	186	0.04	200.10	0.003
Maximum Elevation	Total area lost	186	0.14	428.78	< 0.001

Table 6. Summary of glacier descriptors. TP = Trinity Peninsula. JRI = James Ross Island. VI = Vega Island. IIC = Island Ice Caps. All = all glaciers.

		TP	JRI	VI	IIC	All
Tongue	Grounded	31	24	10	4	69
	Floating	10	16	2	0	28
	Partially Floating	20	16	5	0	41
	Land terminating	1	48	7	0	56
Primary Classification	Ice Cap	11	18	13	4	46
	Ice Field	1	0	0	0	1
	Outlet glacier	27	45	11	0	83
	Valley Glacier	21	16	0	0	37
	Mountain Glacier	1	17	0	0	18
	Glacieret and snowfield	1	8	0	0	9

Table 7. Number of glaciers in each hypsometric class. Categories are from Jiskoot et al. (2009). TP = Trinity Peninsula. JRI = James Ross Island. VI = Vega Island. IIC = Island Ice Caps. All = all glaciers.

Class	Glacier Hypsometry Description	Value	TP	JRI	VI	IIC	All
1	Very bottom heavy	> 1.5	35	42	1	1	79
2	Bottom heavy	$1.2 < HI < 1.49$	7	6	2	0	15
3	Equidimensional	$-1.19 < HI < 1.19$	11	11	4	1	27
4	Top heavy	$-1.2 < HI < -1.49$	1	15	3	0	19
5	Very top heavy	$HI < -1.5$	6	30	14	2	52

Table 8. Number of glaciers advancing and retreating in the period 1988 to 2009. Note that missing data means not all 194 glaciers were included. Glacier change is only noted if it is greater than the mapped error (margin only buffer). "Stationary" glaciers have shown no change greater than the error.

		Number of Glaciers			
		1988–2001		2001–2009	
		No.	%	No.	%
All glaciers	Retreating	160	89.9	146	79.3
	Advancing	8	4.5	3	1.6
	Stationary	9	5.6	35	19.0
	Total	178	100	184	100
Trinity Peninsula	Retreating	51	91.1	52	86.7
	Advancing	4	7.1	0	0
	Stationary	1	1.8	8	13.3
	Total	56	100	60	100
James Ross Island	Retreating	91	91.0	76	73.8
	Advancing	3	3.0	3	2.9
	Stationary	6	6.0	24	23.3
	Total	100	100	103	100
Vega Island	Retreating	14	82.4	15	88.2
	Advancing	1	5.9	0	0.0
	Stationary	2	11.8	2	11.8
	Total	17	100	17	100
Island Ice Caps	Retreating	4	100.0	3	75.0
	Advancing	0	0	0	0
	Stationary	0	0	1	25.0

Table 9. Glacier change, 1988 to 2009. Note there is particularly limited data for 1997. Error margin for 2009 includes errors inherent in polygon determination. As analysis of frontal change in 2001 and 1988 assumes no migration of ice divides, error is calculated by using a 3-pixel wide buffer on either side of the ice front only, and is therefore a minimum error of ice front change only. Where data is missing, it is assumed that the glacier did not change in size between that year and the last year for which data was available; therefore, these figures are a minimum estimate. TP = Trinity Peninsula. JRI = James Ross Island. VI = Vega Island. IIC = Island Ice Caps. All = all glaciers. All area is given in km^2.

Area	Area 2009	Area 2001	Area 1997	Area 1988
All	8140.4 ± 261.7	8414 ± 49.1	8532.1	9460 ± 395.6
TP	5827.3 ± 153.9	5961.6 ± 28.4	5980.3	6689 ± 218.1
JRI	1780.5 ± 86.2	1902.4 ± 15.2	1992.6	2192 ± 136.1
VI	167.8 ± 14.8	169.8 ± 1.2	169.8	178 ± 19.3
IIC	364.7 ± 6.8	380.6 ± 4.8	389.5	400 ± 22.2
Area Lost	2001–2009	1988–2001	1997–2001	1988–2009
All	274.1	1045.5	117.7	1319.5
TP	134.3	727.8	18.7	862.0
JRI	121.9	290.0	90.2	411.9
VI	1.9	8.1	0.00	10.0
IIIC	16.0	19.6	0.00	35.6
Area Gain	2001–2009	1988–2001	1988–2009	
All	0.09	0.08	0.13	
TP	0.00	0.03	0.03	
JRI	0.06	0.05	0.10	
VI	0.00	0.00	0.00	
IIC	0.00	0.00	0.00	

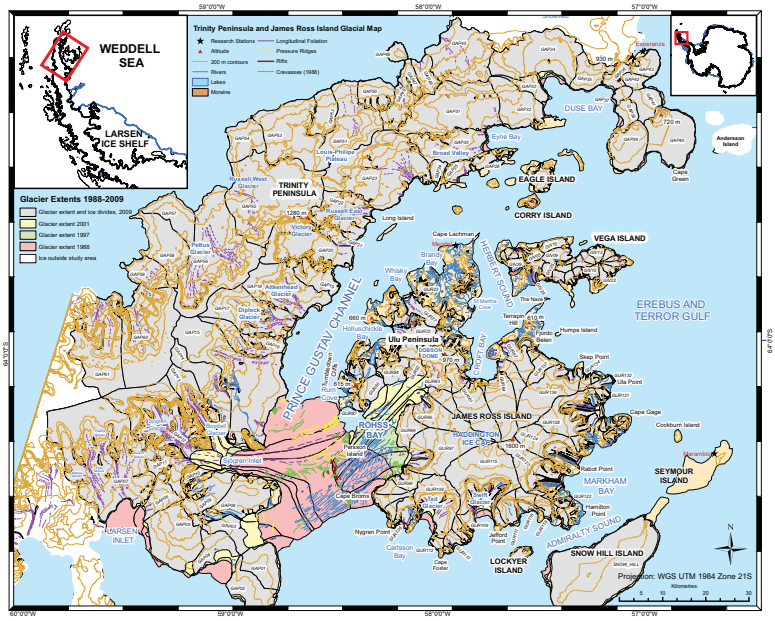

Fig. 1. Index map of James Ross Island, Vega Island, Snow Hill Island and Trinity Peninsula, Northern Antarctic Peninsula, showing ice divides, glacier drainage basins and glacier ID codes. Glacier extents in 2009, 2001, 1997 and 1988 are shown. Remotely-sensed images (refer to Supplement) used in making this map and all subsequent maps were projected in the Universal Transverse Mercator (UTM) projection World Geodetic System (WGS) 1984 Zone 21S.

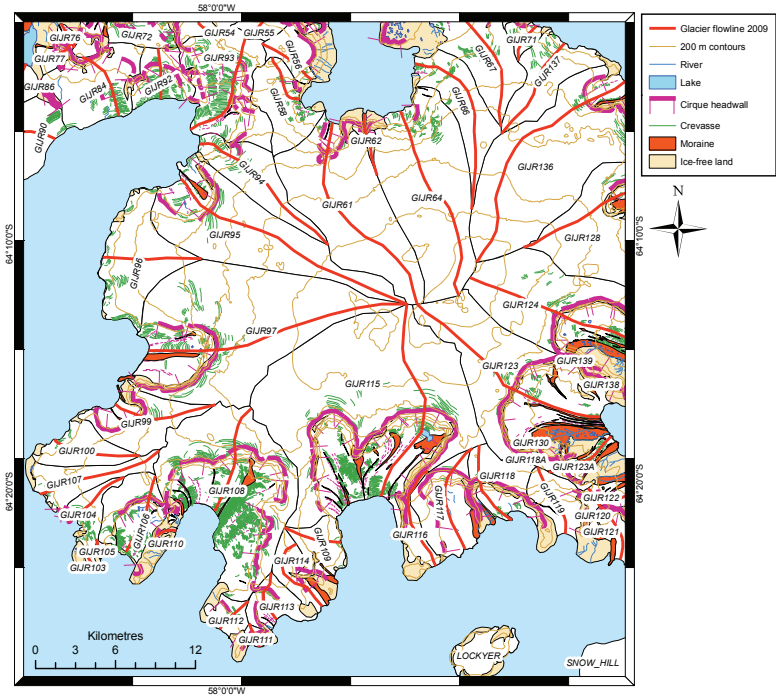

Fig. 2. Subset of the glaciological map for James Ross Island, showing mapped *Length* in 2009 along the centre line of each glacier drainage basin. In the accumulation area, *Length* follows the steepest downhill gradient; in the accumulation area, it follows the centre line as closely as possible. *Length* was measured from the highest to the lowest point on the glacier polygon.

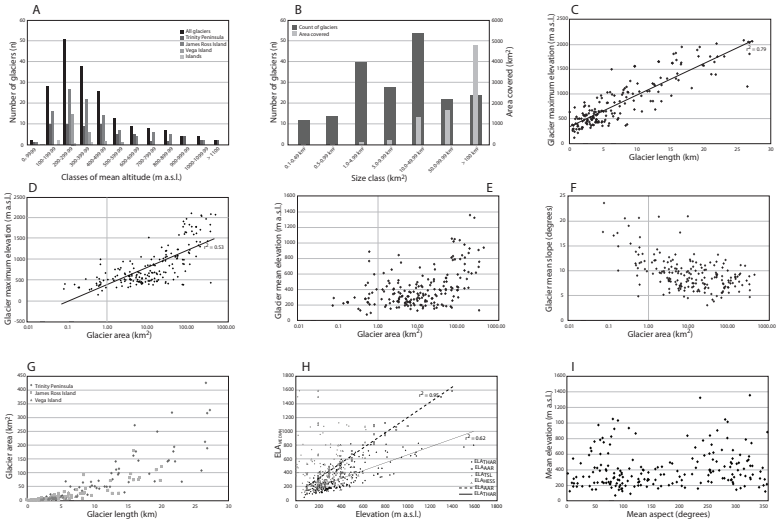

Fig. 3. **(A)** Number of glaciers with different mean elevations, separated according to region. **(B)** Frequency distribution of different glacier area classes, compared with total area covered by each size class. **(C)** Scatter plot showing a strong relationship ($r^2 = 0.8$) between glacier maximum elevation and glacier length. **(D)** Relationship between maximum elevation and area ($r^2 = 0.5$). **(E)** Scatter plot showing a weak relationship between mean elevation and glacier area. **(F)** Scatter plot showing a weak relationship between mean slope and log glacier area. **(G)** Scatter plot showing a strong relationship between glacier area and glacier length. **(H)** Correlation between ELA_{MEDIAN} and different methods of ELA calculation. **(I)** Relationship between mean aspect and mean elevation. See Table 5 for *p* values.

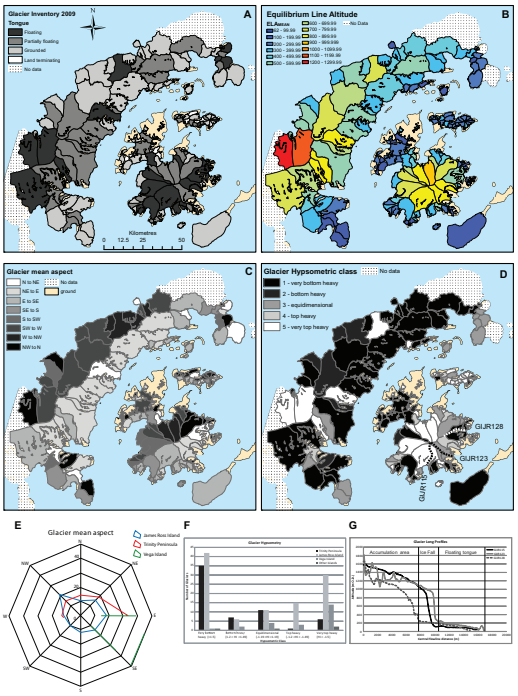

Fig. 4. **(A)** Distribution of floating, partially floating and grounded glacier tongues at glacier termini. **(B)** Mean ELA for each glacier polygon. Glaciers in red have the highest ELA_{MEAN}, while glaciers in dark blue have ELA_{MEAN} close to 100 m. **(C)** Mean aspect of the glacier polygons. **(D)** Distribution of glacier hypsometric classes. **(E)** Percentages of glaciers in each cardinal direction. **(F)** Frequency distribution of glaciers with different hypsometric indices in different regions. **(G)** Long profiles of three tidewater glaciers on James Ross Island.

Fig. 5. Normalised hypsometric curves of representative tidewater glaciers on Trinity Peninsula and James Ross Island. Hypsometric Index (HI) and mean equilibrium line altitude (ELA_{MEAN}) are given in the top right hand corner for each glacier graph. The normalised ELA_{MEAN} for each glacier is plotted. ELA_{2C} indicates the possible change in equilibrium line with future climate change. A 2 °C warming could result (presuming an adiabatic lapse rate of −5.8 °C/1000 m) in a rise in ELA of 345 m by 2040.

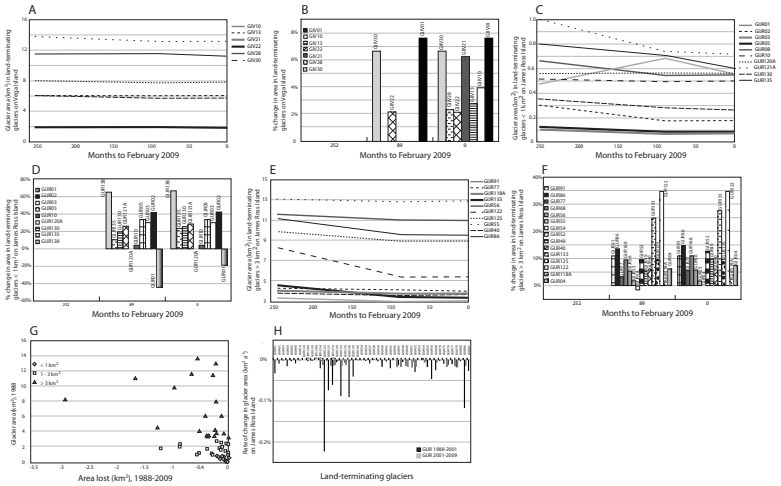

Fig. 6. **(A)** Percentage change in surface area for land-terminating glaciers on Vega Island. Many glaciers receded after 1997 and 2001. **(B)** Recession over time of land-terminating glaciers on Vega Island. **(C)** Percentage change for small land-terminating glaciers (less than 1 km^2) on James Ross Island. **(D)** Glacier change for small land-terminating glaciers on James Ross Island. **(E)** Percentage change for land-terminating glaciers > 3 km^2 on James Ross Island. **(F)** Glacier change for and-terminating glaciers (greater than 3 km^2) on James Ross Island. **(G)** Scatter plot demonstrating a weak correlation between change in glacier area and initial glacier size ($r^2 = 0.11$; see Table 5). **(H)** Variance in rates of change for land-terminating glaciers on James Ross Island.

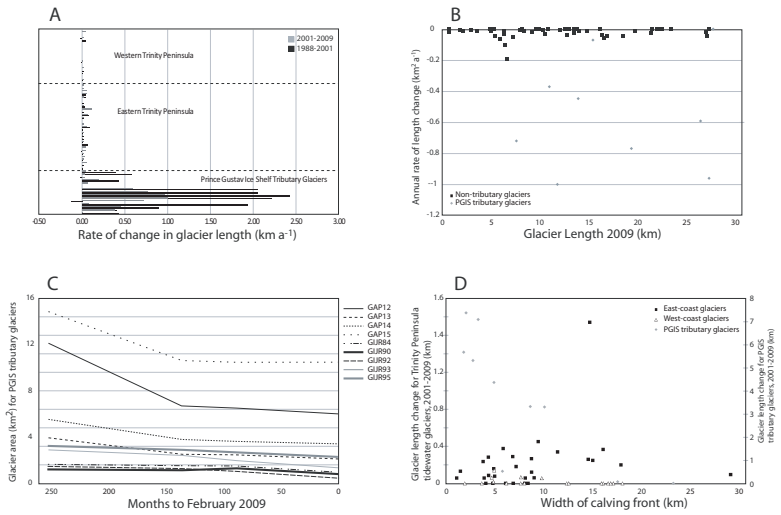

Fig. 7. Tidewater glacier length. **(A)** Rates of glacier length change in tidewater glaciers on Trinity Peninsula. **(B)** Scatter plot showing poor correlation between 2009 glacier length and length changes. **(C)** Chart illustrating change in glacier area for tributary glaciers to Prince Gustav Ice Shelf. Note that most change occurred prior to 2001. **(D)** Scatter plot showing poor correlation between the width of the calving front and the change in glacier length.

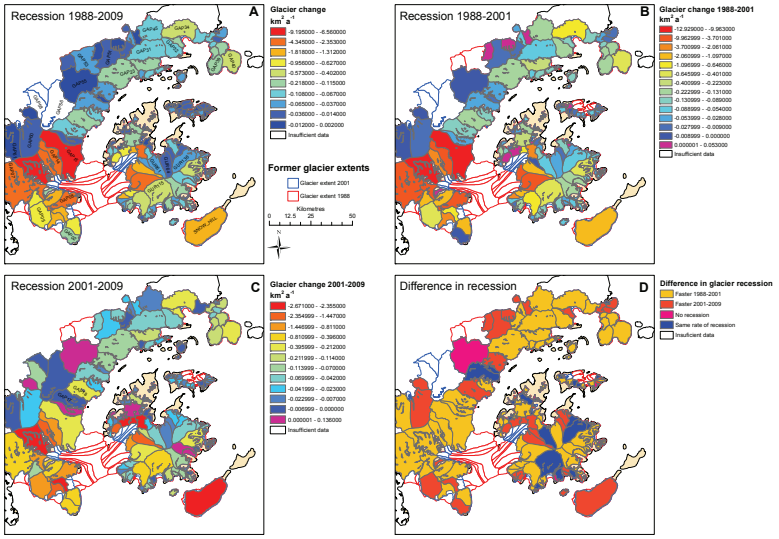

Fig. 8. Annualised rates of recession for different time periods. Glaciers in red retreated fastest, and glaciers in dark blue had the slowest annual recession rates. Glaciers in pink advanced. Recession category values are determined by Natural Breaks (Jenks) method. **(A)** Overall glacier recession, 1988–2009. Note the slow rates of recession on Western Trinity Peninsula. **(B)** Glacier rates of recession, 1988–2001. PGIS tributary glaciers retreated fastest. Note that two PGIS-tributary glaciers in Röhss Bay advanced during this period (coloured purple). **(C)** Glacier rates of recession, 2001–2009. Note a few small advancing glaciers (coloured purple). **(D)** Difference in recession rates. Glaciers in blue retreated fastest between 1988 and 2001; glaciers in red retreated fastest after 2001. Note that PGIS tributary glaciers retreated slower after 2001.